hematoxylin and eosin; IVIg: intravenous immunoglobulin; KD: Kawasaki disease; MLR: mixed lymphocytes reaction method; MZR: mizoribine; NOS: Nitrous Oxide Systems: PBS; Dulbecco's phosphate- buffered saline; SG: saline containing 0.1% glucose.

Contribution of authors

KT: Histological evaluations of coronary arteritis. TO: Histological evaluations of coronary arteritis. TN: Measurement and analysis of cytokines and chemokines. YY: Measurement and analysis of cytokines and chemokines. HY: Histological evaluations of coronary arteritis. NNM: Preparation of CAWS. NO: Preparation of CAWS. TS: Planning treatments with MZR and IgG, and clinical evaluation. TO: Planning treatments with MZR and IgG, and clinical evaluation. KS: Measurement and analysis of cytokines and chemokines, correspondence to all evaluation of this study. All authors read and approved the final manuscript.

Acknowledgements

We thank Dr. Shiro Naoe (Department of Biomedical Engineering, Toin University of Yokohama, Yokohama). We are also grateful to Mr. Kazuo Tomizawa of NIID for excellent assistance with animal experiments.

Author details

[1]Department of Pathology, Toho University Ohashi Medical Center, Meguro-ku, Tokyo, 153-8515, Japan. [2]Inflammation Program, Dept. of Immunology, Chiba University Graduate School of Medicine, Chuo-ku, Chiba, 260-8670, Japan. [3]Laboratory for Immunopharmacology of Microbial Products, School of Pharmacy, Tokyo University of Pharmacy and Life Science, Hachioji, Tokyo 192-0392, Japan. [4]Department of Pediatrics, Toho University Omori Medical Center, Ota-ku, Tokyo, 143-8541, Japan. [5]Kure Kyosai Hospital, Kure, Hiroshima, 737-8505, Japan.

Competing interests

The authors declare that they have no competing interests.

Received: 3 April 2011 Accepted: 29 September 2011
Published: 29 September 2011

References

1. Kawasaki T: **Acute febrile muco-cutaneous lymph node syndrome in young children with unique digital desquamation.** *Jpn J Allergol* 1967, **16**:178-222.
2. Kawasaki T, Kosaki F, Okawa S, Shigematsu I, Yanagawa H: **New infantile acute febrile mucocutaneous lymph node syndrome (MLNS) prevailing in Japan.** *Pediatrics* 1974, **54**:271-276.
3. Furusho K, Sato K, Soeda T, Matsumoto H, Okabe T, Hirota T, Kawada S: **High-dose intravenous gammaglobulin for Kawasaki disease.** *Lancet* 1983, **10(8363)**:1359.
4. Nakamura Y, Yashiro M, Uehara R, Sadakane A, Chihara I, Aoyama Y, Kotani K, Yanagawa H: **Epidemiologic features of Kawasaki disease in Japan: results of the 2007-2008 nationwide survey.** *J Epidemiol* 2010, **20**:302-307.
5. Sundel RP, Burns JC, Baker A, Beiser AS, Newburger JW: **Gamma globulin re-treatment in Kawasaki disease.** *J Pediatr* 1993, **123**:657-659.
6. Shinohara M, Sone K, Tomomasa T, Morikawa A: **Corticosteroids in the treatment of the acute phase of Kawasaki disease.** *J Pediatr* 1999, **135**:465-469.
7. Kobayashi T, Inoue Y, Takeuchi K, Okada Y, Tamura K, Tomomasa T, Kobayashi T, Morikawa A: **Prediction of intravenous immunoglobulin unresponsiveness in patients with Kawasaki disease.** *Circulation* 2006, **113**:2606-2612.
8. Villain E, Kachaner J, Sidi D, Blaysat G, Piéchaud JF, Pedroni E: **Trial of prevention of coronary aneurysm in Kawasaki's disease using plasma exchange or infusion of immunoglobulins.** *Arch Fr Pediatr* 1987, **44**:79-83.
9. Imagawa T, Mori M, Miyamae T, Ito S, Nakamura T, Yasui K, Kimura H, Yokota S: **Plasma exchange for refractory Kawasaki disease.** *Eur J Pediatr* 2004, **163**:263-264.
10. Mori M, Imagawa T, Katakura S, Miyamae T, Okuyama K, Ito S, Nakamura T, Kimura H, Yokota S: **Efficacy of plasma exchange of plasma exchange therapy for Kawasaki disease intractable to intravenous gamma-globulin.** *Mod Rheumatol* 2004, **14**:43-47.
11. Wright DA, Newburger JW, Baker A, Sundel RP: **Treatment of immune globulin-resistant Kawasaki disease with pulsed doses of corticosteroids.** *J Pediatr* 1996, **128**:146-149.
12. Wallace CA, French JW, Kahn SJ, Sherry DD: **Initial intravenous gammaglobulin treatment failure in Kawasaki disease.** *Pediatrics* 2000, **105**:E78.
13. Zaitsu M, Hamasaki Y, Tashiro K, Matsuo M, Ichimaru T, Fujita I, Tasaki H, Miyazaki S: **Ulinastatin, an elastase inhibitor, inhibits the increased mRNA expression of prostaglandin H2 synthase-type 2 in Kawasaki disease.** *J Infect Dis* 2000, **181**:1101-1109.
14. Miura M, Ohki H, Tsuchihashi T, Yamagishi H, Katada Y, Yamada K, Yamashita Y, Sugaya A, Komiyama O, Shiro H: **Coronary risk factors in Kawasaki disease treated with additional gammaglobulin.** *Arch Dis Child* 2004, **89**:776-780.
15. Uehara R, Yashiro M, Oki I, Nakamura Y, Yanagawa H: **Re-treatment regimens for acute stage of Kawasaki disease patients who failed to respond to initial intravenous immunoglobulin therapy: analysis from the 17th nationwide survey.** *Pediatr Int* 2007, **49**:427-430.
16. Iwashima S, Seguchi M, Matubayashi T, Ohzeki T: **Ulinastatin therapy in Kawasaki disease.** *Clin Drug Investig* 2007, **27**:691-696.
17. Raman V, Kim J, Sharkey A, Chatila T: **Response of refractory Kawasaki disease to pulse steroid and cyclosporine A therapy.** *Pediatr Infect Dis* 2001, **20**:635-637.
18. Adachi S, Sakaguchi H, Kuwahara T, Uchida Y, Fukao T, Kondo N: **High regression rate of coronary aneurysms developed in patients with immune globulin.** *Tohoku J Exp Med* 2010, **220**:285-290.
19. Weiss JE, Eberhard BA, Chowdhury D, Gottlieb BS: **Infliximab as a novel therapy for refractory Kawasaki disease.** *J Rheumatol* 2004, **31**:808-810.
20. Saji T, Kemmotsu Y: **Infliximab for Kawasaki syndrome [reply].** *J Pediatr* 2006, **149**:426.
21. Burns JC, Best BM, Mejias A, Mahony L, Fixler DE, Jafri HS, Melish ME, Jackson MA, Asmar BI, Lang DJ, Connor JD, Capparelli EV, Keen ML, Mamun K, Keenan GF, Ramilo O: **Infliximab treatment of intravenous immunoglobulin-resistant Kawasaki disease.** *J Pediatr* 2008, **153**:833-838.
22. Shirley DA, Stephens I: **Primary treatment of incomplete Kawasaki disease with infliximab and methylprednisolone in a patient with a contraindication to intravenous immune globulin.** *Pediatr Infect Dis J* 2010, **29**:978-979.
23. Son MB, Gauvreau K, Burns JC, Corinaldesi E, Tremoulet AH, Watson VE, Baker A, Fulton DR, Sundel RP, Newburger JW: **Infliximab for intravenous immunoglobulin resistance in Kawasaki disease: a retrospective study.** *J Pediatr* 2011, **158**:644-649.
24. Ishikawa H: **Mizoribine and mycophenolate mofetil.** *Curr Medicinal Chem* 1999, **6**:575-597.
25. Yokota S: **Mizoribine: Mode of action and effects in clinical use.** *Pediatr Int* 2002, **44**:196-198.
26. Kawasaki Y, Hosoya M, Suzuki J, Onishi N, Takahashi A, Isome M, Nozawa R, Suzuki H: **Efficacy of multidrug therapy combined with mizoribine in children with diffuse IgA nephropathy in comparison with multidrug therapy without mizoribine and with methylprednisolone pulse therapy.** *Am J Nephrol* 2004, **24**:576-581.
27. Yoshikawa N, Nakanishi K, Ishikura K, Hataya H, Iijima K, Honda M: **Japanese Pediatric IgA Nephropathy Treatment Study Group: combination therapy with mizoribine for severe childhood IgA nephropathy: a pilot study.** *Pediatr Nephrol* 2008, **23**:757-763.
28. Honda M: **Nephrotic syndrome and mizoribine in children.** *Pediatr Int* 2002, **44**:210-216.
29. Hirayama K, Kobayashi M, Hashimoto Y, Usui J, Shimizu Y, Hirayama A, Yoh K, Yamagata K, Nagase S, Nagata M, Koyama A: **Treatment with the purine synthesis inhibitor mizoribine for ANCA-associated renal vasculitis.** *Am J Kidney Dis* 2004, **44**:57-63.

30. Ohtomo Y, Fujinaga S, Takada M, Murakami H, Akashi S, Shimizu T, Kaneko K, Yamashiro Y: **High-dose mizoribine therapy for childhood-onset frequently relapsing steroid-dependent nephritic syndrome with cyclosporine nephrotoxicity.** *Pediatr Nephrol* 2005, **20**:1744-1749.
31. Takahashi K, Oharaseki T, Wakayama M, Yokouchi Y, Naoe S, Murata H: **Histopathological features of murine systemic vasculitis caused by *Candida albicans* extract - an animal model of Kawasaki disease.** *Inflamm Res* 2004, **53**:72-77.
32. Okubo M, Chen XM, Kamata K, Masaki Y, Uchiyama T: **Suppressive effect of mizoribine on humoral antibody production in DBA/2 mice.** *Transplantation* 1986, **41**:495-498.
33. Takahashi K, Oharaseki T, Nagai-Miura N, Ohno N, Ishida-Okawara A, Yamada H, Kaneshiro Y, Naoe S, Suzuki K: **Administration of human immunoglobulin inhibited development of vasculitis in a murine model of vasculitis induced with CAWS, *Candida albicans* water soluble fraction.** *Modern Reumatol* 2010, **20**:160-167.
34. Tomizawa K, Nagao T, Kusunoki R, Saiga K, Oshima M, Kobayashi K, Nakayama T, Tanokura M, Suzuki K: **Reduction of MPO-ANCA epitopes in SCG/Kj mice by 15-deoxyspergualin treatment restricted by IgG2b associated with crescentic glomerulonephritis.** *Rheumatology (Oxford)* 2010, **49**:1245-1256.
35. Jibiki T, Terai M, Kohno Y: **High concentrations of interleukin-8 and monocyte chemoattractant protein-1 in urine of patients with acute Kawasaki disease.** *Eur J Pediatr* 2004, **163**:749-750.
36. Oharaseki T, Kameoka Y, Kura F, Persad AS, Suzuki K, Naoe S: **Susceptibility loci to coronary arteritis in animal model of Kawasaki disease induced with *Candida albicans*-derived substances.** *Microbiol Immunol* 2005, **49**:181-189.
37. Nagi-Miura N, Shingo Y, Adachi Y, Ishida-Okawara A, Oharaseki T, Takahashi K, Naoe S, Suzuki K, Ohno N: **Induction of coronary arteritis with administration of CAWS (Candida albicans water-soluble fraction) depending on mouse strains.** *Immunopharmacol Immunotoxicol* 2004, **26**:527-543.
38. Koyama H, Tsuji M: **Genetic and biochemical studies on the activation and cytotoxic mechanism of bredinine, a potent inhibitor of purine biosynthesis in mammalian cells.** *Biochem Pharmacol* 1983, **32**:3547-3553.
39. Gan L, Mohammad R, Seyedsayamdost , Shuto S, Matsuda A, Gregory A, Hedstrom PL: **The immunosuppressive agent mizoribine monophosphate forms a transition state analogue complex with inosine monophosphete dehydrogenase.** *Biochemistry* 2003, **42**:857-863.
40. Kusumi T, Tsuda M, Katsunuma T, Yamamura M: **Dual inhibitory effect of bredinin.** *Cell Biochem Func* 1988, **7**:201-204.
41. Kikuchi Y, Imakiire T, Yamada M, Saigusa T, Hyodo T, Hyodo N, Suzuki S, Miura S: **Mizoribine reduces renal injury and macrophage infiltration in non-insulin-dependent diabetic rats.** *Nephrol Dial Transplant* 2005, **20**:1573-1581.
42. Ikezumi Y, Suzuki T, Karasawa T, Hasegawa H, Kawachi H, Nikolic-Paterson DJ, Uchiyama M: **Contrasting effects of steroids and mizoribine on macrophage activation and glomerular lesions in rat Thy-1 mesangial proliferative glomerulonephritis.** *Am J Nephrol* 2010, **31**:273-282.
43. Sonda K, Takahashi K, Tanabe K, Funchinoue S, Hayasaka Y, Kawaguchi H, Teraoka S, Toma H: **Clinical pharmacokinetic study of mizoribine in renal transplantation patients.** *Transplant Proc* 1996, **28**:3643-3648.
44. Turka LA, Dayton J, Sinclair G, Thompson CB, Mitchell BS: **Guanine ribonucleotide depletion inhibits T cell activation.** *J Clin Invest* 1991, **87**:940-948.

doi:10.1186/1546-0096-9-30
Cite this article as: Takahashi *et al.*: Mizoribine provides effective treatment of sequential histological change of arteritis and reduction of inflammatory cytokines and chemokines in an animal model of Kawasaki disease. *Pediatric Rheumatology* 2011 **9**:30.

Molecular Immunology 48 (2011) 1191–1202

Contents lists available at ScienceDirect

Molecular Immunology

journal homepage: www.elsevier.com/locate/molimm

Free heme is a danger signal inducing expression of proinflammatory proteins in cultured cells derived from normal rat hearts

Kazuhisa Hao[a], Haruo Hanawa[a,*], Limin Ding[a], Yoshimi Ota[b], Kaori Yoshida[a], Ken Toba[a], Minako Ogura[a], Hiromi Ito[a], Makoto Kodama[a], Yoshifusa Aizawa[a]

[a] Division of Cardiology, Niigata University Graduate School of Medical and Dental Sciences, 1-757 Asahimachi-dori, Niigata 951-8120, Japan
[b] Department of Medical Technology, School of Health Sciences, Faculty of Medicine, Niigata University, Niigata, Japan

ARTICLE INFO

Article history:
Received 10 November 2010
Received in revised form 7 February 2011
Accepted 28 February 2011
Available online 5 April 2011

Keywords:
Inflammation
Macrophages
Oxidative stress
Cytokines
Chemokines

ABSTRACT

Endogenous molecules from damaged tissue act as danger signals to trigger or amplify the immune/inflammatory response. In this study, we examined whether free heme induced pro-inflammatory proteins in cultured cells derived from normal hearts and investigated the cells targeted by heme, together with its mechanism of action in these cells. We cultured collagenase-isolated heart-derived cells from normal rats and examined whether free heme induced pro-inflammatory proteins, reactive oxygen species (ROS) production and NF-κB activation, by quantitative RT-PCR, ELISA and flow cytometry. Free heme increased mRNA of various pro-inflammatory proteins in cultured cardiac resident cells (CCRC) (at least 100-fold) and induced intracellular ROS formation. Approximately 85–90% of CCRC are fibroblast/smooth muscle cells and 10–15% are CD11bc-positive macrophages; therefore to examine individual target cells, macrophage-deleted (CD11bc-negative) CCRC, primary cultured cells (cardiac fibroblasts, arterial smooth muscle cells and cardiac microvascular endothelial cells) and macrophage cells lines (NR8383) were similarly treated. Free heme activated NF-κB and induced expression of some pro-inflammatory proteins, including IL-1 and TNF-α in NR8383. On the other hand, macrophage-deleted CCRC strongly increased expression of these proteins on treatment with IL-1 or TNF-α, but not free heme. Induction of expression of pro-inflammatory proteins by free heme was not inhibited by intracellular ROS reduction, but by protease and proteasome inhibitors capable of regulating NF-κB. These data suggest that free heme strongly induces various pro-inflammatory proteins in injured hearts through NF-κB activation in cardiac resident macrophages and through cross-talk between macrophages and fibroblast/smooth muscle cells mediated inter alia by IL-1, TNF-α.

1. Introduction

In response to cardiac injury, resident cells such as cardiomyocytes, endothelial cells, pericytes, smooth muscle cells, fibroblasts, mast cells and resident macrophages are thought to rapidly react to environmental changes and cross-talk mediated by various mediators (Frangogiannis, 2008; Yoshida et al., 2005). Recent reports have indicated that endogenous intracellular contents released by dying cells initiate an intense inflammatory response by activating the innate immune mechanism. Heat shock proteins (Chen et al., 1999), hyaluronan (Scheibner et al., 2006), fibronectin fragments (Okamura et al., 2001) and uric acid (Shi et al., 2003) serve as "danger signals" that trigger an inflammatory cascade. Even in the absence of microbial pathogens, "danger signals" can activate the innate immune system (Frantz et al., 2007; Shi et al., 2003; Trendelenburg, 2008). However, the identity of "danger signals" in myocardium remains largely unknown; nor is it known which resident cells react to these signals and produce pro-inflammatory proteins such as cytokines and chemokines.

On the other hand, our previous gene expression analysis in hearts of rats with myocarditis by DNA microarray and real time RT-PCR has demonstrated that gene expression of several iron metabolism-related proteins, such as lipocalin-2/NGAL/alpha-2μ globulin-related protein (Lcn2/NGAL), hepcidin and heme oxygenase-1 (HO-1), is markedly increased in such cardiomyocytes (Ding et al., 2010; Isoda et al., 2010; Watanabe et al., 2008). The role of these proteins in injured hearts still remains largely unknown; however, this finding led us to hypothesize that resident cells in injured hearts are rapidly and strongly influenced by a molecule

Abbreviations: CCRC, cultured cardiac resident cells; CRC, cardiac resident cells; EAM, experimental autoimmune myocarditis; HO-1, heme oxygenase-1; IL-1, interleukin-1; Lcn2, lipocalin-2; ROS, reactive oxygen species; RASMC, rat aortic smooth muscle cells; RCF, rat cardiac fibroblasts; RHMVEC, rat heart microvascular endothelial cells; TLCK, Tosyl-Lys-chloromethylketone; TPCK, Tosyl phenylalanyl chloromethyl ketone.

* Corresponding author. Tel.: +81 25 227 2185; fax: +81 25 227 0774.
E-mail address: hanawa@med.niigata-u.ac.jp (H. Hanawa).

0161-5890/$ – see front matter © 2011 Elsevier Ltd. All rights reserved.
doi:10.1016/j.molimm.2011.02.013

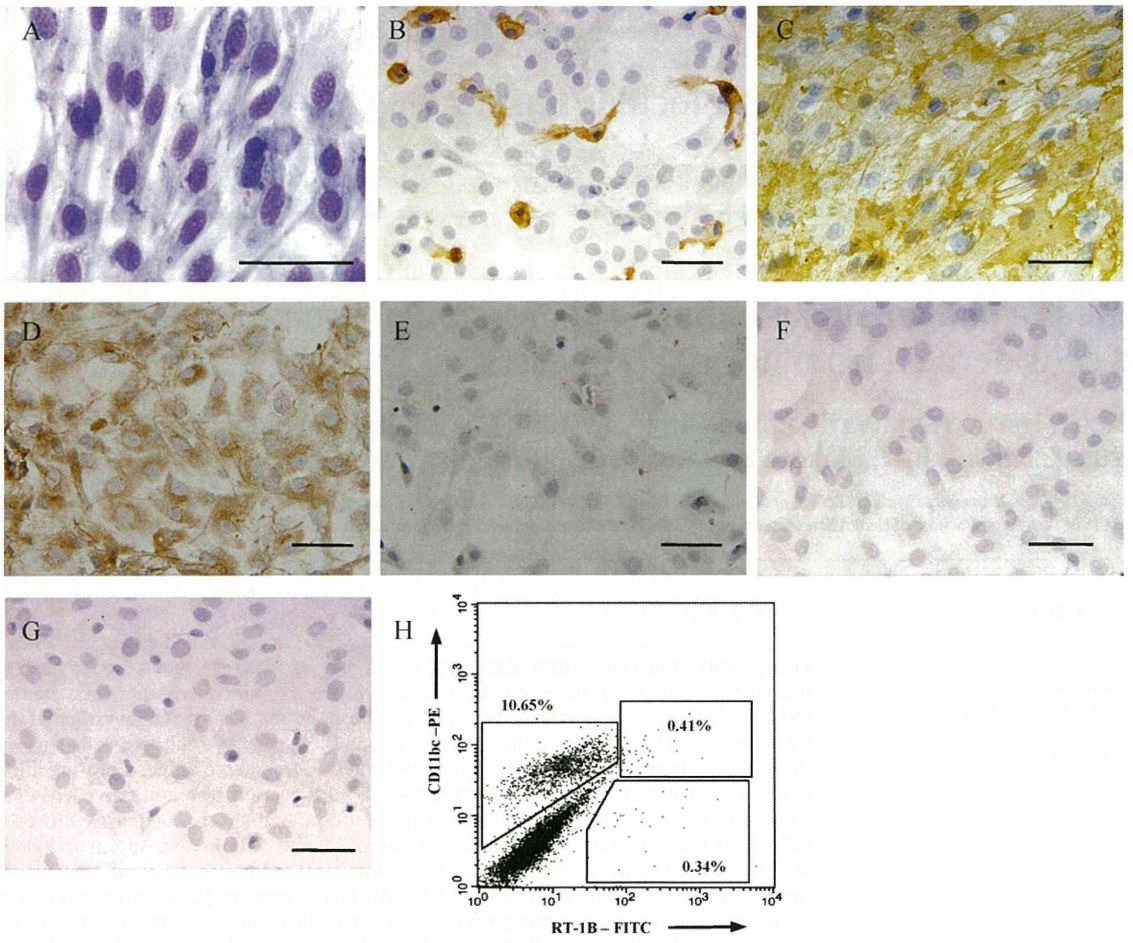

Fig. 1. Immunohistochemical staining and flow cytometry of CCRC from normal hearts. CCRC were isolated from the hearts of 8-week old normal rats and cultured for 2 weeks on chamber slides. (A) May-Giemsa stain, (B) CD11bc, (C) α-smooth muscle actin, (D) collagen type III, (E) factor VIII-related Ag, (F) rabbit serum as a negative control, (G) mouse IgG2a as a negative control, and (H) flow cytometry of CCRC. Bar represents 50 μm.

containing iron, which is critically involved in inflammation. In other words, it has been speculated that this may be one of the "danger signals" released from damaged cardiac tissue. In fact, cardiomyocytes are a cell type containing a large amount of iron (Brown et al., 2007). Cardiomyocytes must maintain high intracellular oxygen levels to generate sufficient energy for contraction and relaxation (Wittenberg and Wittenberg, 1987); therefore, cardiomyocytes possess high levels of myoglobin containing heme (iron protoporphyrin IX), which is involved in oxygen storage and facilitation of oxygen diffusion to the mitochondria (Wittenberg and Wittenberg, 2003). On the other hand, serum myoglobin is also a biomarker for the early detection of myocardial infarction (Stone et al., 1975). This means that, in case of cardiac injury, myoglobin is released into the extracellular space and leaks into the circulation. Moreover, it suggests that dispersed myoglobin is partially degraded in cardiac lesions, thereby increasing the concentration of free heme at the site of damage (Nakahira et al., 2003). Because free heme is highly lipophilic, it will rapidly intercalate into the lipid membranes of adjacent cells (Beri and Chandra, 1993). Recent studies have revealed that free heme is a potent pro-oxidant by virtue of its ability to promote reactive oxygen species (ROS) formation (Hasan and Schafer, 2008); furthermore, ROS are involved in interleukin-1 (IL-1)β production by triggering inflammasome signaling (Allen et al., 2009; Cruz et al., 2007). Moreover, free heme has also been reported to induce the expression of pro-inflammatory adhesion molecules both on endothelium and blood cells (Wagener et al., 1997, 2001), monocyte chemoattractant protein (MCP)-1 in immortalized proximal tubular cells (Kanakiriya et al., 2003) and tumor necrosis factor (TNF)-α in peritoneal macrophages (Figueiredo et al., 2007). Free heme is a major regulator of gene expression (Tsiftsoglou et al., 2006).

For these reasons, we here investigated whether ferriprotoporphyrin IX (hemin), into which heme released from globin is converted by iron oxidation in the presence of chloride ions (Tsiftsoglou et al., 2006), induced pro-inflammatory proteins in heart. Approximately 75% of the total cell number in normal heart is considered to be non-cardiomyocytes in the interstitium (Zak, 1973) and the majority are fibroblasts (Eghbali et al., 1988). On the other hand, recent studies have suggested that tissue resident macrophages react to endogenous products of damaged cells and tissues (Medzhitov, 2008; Zitvogel et al., 2010). In this study, we have investigated the influence of hemin on cultured cardiac resident cells (CCRC) with cardiac resident macrophages and fibroblasts.

2. Materials and methods

2.1. Conditions for culture of cardiac resident cells

Cardiac resident cells (CRC) were isolated by forcing aseptically well-washed hearts of 8-week-old normal male Lewis rats through a 200-gauge stainless steel mesh after trypsin and collagenase digestion using 0.25% trypsin–EDTA solution (Invitrogen Life Technologies, Tokyo, Japan) plus 0.0075% collagenase Type

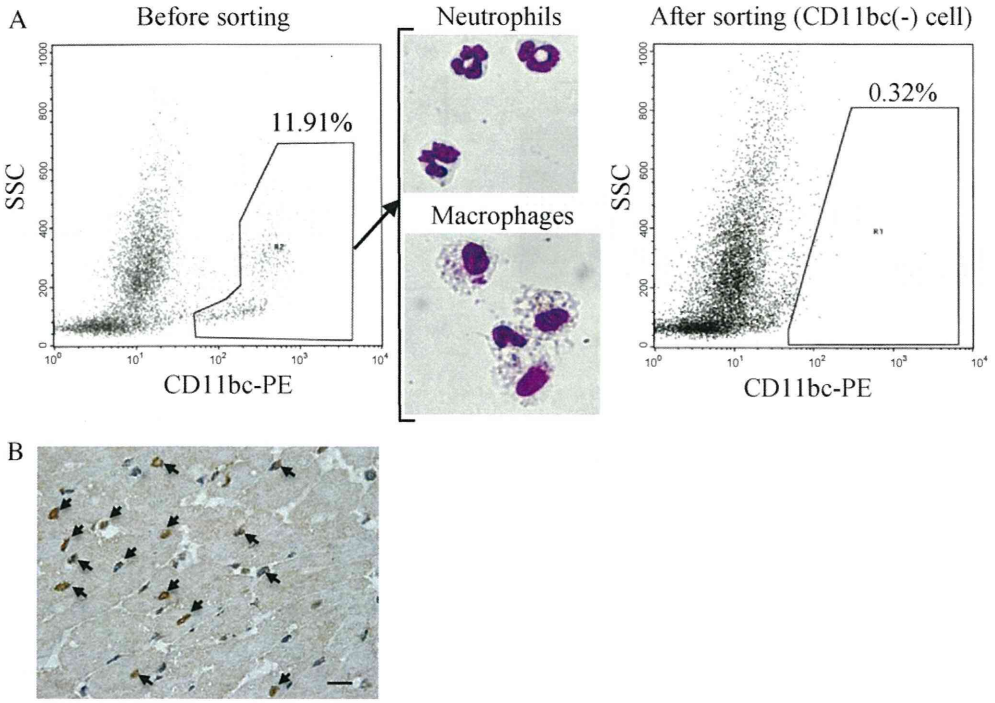

Fig. 2. Flow cytometric and cytospin analyses (A) of CRC from normal hearts before and after sorting of CD11bc-positive cells and immunohistochemical staining of a normal heart (B). (A) CD11bc-positive cells of CRC were removed by a MACS magnetic cell sorting system (from 11.91% to 0.32%). Cytospin preparations of CD11bc-positive cells revealed that they were granulocytes (approximately 40%) and macrophage-like cells (approximately 60%). (B) CD11bc immunostaining of a normal heart. CD11bc-positive cells (arrows). Bar represents 10 μm.

II (Invitrogen), at 37 °C for 20 min. Cells were then hemolyzed in 0.17 M Tris buffer supplemented with 0.83% NH_4Cl and were separated by passing through 125 μm stainless steel sieves to remove necrotic debris. CRC were cultured for 2–3 weeks on 35-mm-well dishes in 2 ml RPMI medium supplemented with 10% heat-inactivated FBS, 100 unit/ml penicillin, and 100 μg/ml streptomycin. These were the cultured CRC (CCRC) used for hemin-stimulation experiments. CD11bc-negative CCRC were prepared as follows. The above-described CRC were separated using PE-conjugated CD11bc (OX-42) (Pharmingen, San Diego, CA), anti-PE micro beads (Miltenyi Biotec, Bergisch Gladbach, Germany) and a MACS magnetic cell sorting system (Miltenyi Biotec). CD11bc-positive and -negative CRC were confirmed by flow cytometry and CD11bc-positive CRC were used for cytospin preparations to examine morphology. CD11bc-negative CRC were purified for culture as follows: Cells were cultured for 2–3 weeks on 35-mm-well dishes in the above-mentioned medium and were used as CD11bc-negative CCRC for hemin-stimulation experiments. Cultured cells for experiments were maintained by changes of the above-described media every 3–4 days until 80–90% confluent.

2.2. Culture of primary cells and cell lines

Primary rat aortic smooth muscle cells (RASMC) (VEC Technologies Inc., Rensselaer, NY) and primary rat heart microvascular endothelial cells (RHMVEC) (VEC Technologies Inc.) were maintained in CS-C Medium Kits R (DS Pharma Biomedical Co. Osaka, Japan) and primary rat cardiac fibroblasts (RCF) were maintained in rat fibroblast growth medium (CELL Applications Inc.). The rat NR8383 macrophage cell line (American Type Culture Collection, Manassas, VA) was maintained in Ham's F12K medium with 2 mM L-glutamine and 15% heat-inactivated FBS, 100 unit/ml penicillin and 100 μg/ml streptomycin. Cultured cells for experiments were maintained by changes of the above-described media every 3–4 days until 80–90% confluent.

2.3. Flow cytometry

Direct staining of CCRC, CRC before sorting and CD11bc-negative CRC immediately after sorting was carried out with phycoerythrin (PE)-conjugated mouse monoclonal antibodies against rat CD11bc (clone OX-42) (BD Pharmingen), fluorescein isothiocyanate (FITC)-conjugated mouse monoclonal antibodies against rat RT1B (MHC class II antigen, I-A) (OX-6) (BD Pharmingen); cells were then analyzed using a FACScan flow cytometer (Becton Dickinson).

2.4. Stimulation and inhibition of cultured cells

Stock solutions of hemin (iron protoporphyrin chloride) (Sigma–Aldrich, St. Louis, MO) were prepared in 0.01 N NaOH. CCRC ($n=4$), CD11bc-negative CCRC ($n=4$), primary cells ($n=4$) and NR8383 ($n=4$) were stimulated with hemin and harvested sequentially over the following 24 h. Lipopolysaccharide (LPS) was purchased from Sigma–Aldrich. The superoxide scavenger Tiron (4,5-dihydroxy-1,3-benzenedisulfonic acid, 10 mM) (Sigma–Aldrich) was added 3 h before hemin-stimulation. The proteinase inhibitors, Tosyl phenylalanyl chloromethyl ketone (TPCK, 25 μM) (Sigma–Aldrich), Tosyl-Lys-chloromethylketone (TLCK, 300 μM) (Sigma–Aldrich) and the proteasome inhibitor, Bortezomib (10 μM) (Toronto Research Chemicals, North York, Canada), which also act as NF-κB inhibitors, were added 1 h before hemin. CD11bc-negative CCRC ($n=4$) were stimulated with 2.5 ng/ml rat IL-1α (Peprotech, London, UK) and 10 ng/ml rat TNF-α (R&D Systems, Minneapolis, MN) and harvested sequentially over the following 24 h.

2.5. Real-time polymerase chain reaction

Total RNA was isolated from the materials described above using Trizol (Invitrogen, Tokyo, Japan). cDNA was synthesized from 2 to 5 μg of total RNA with random primers and murine Moloney

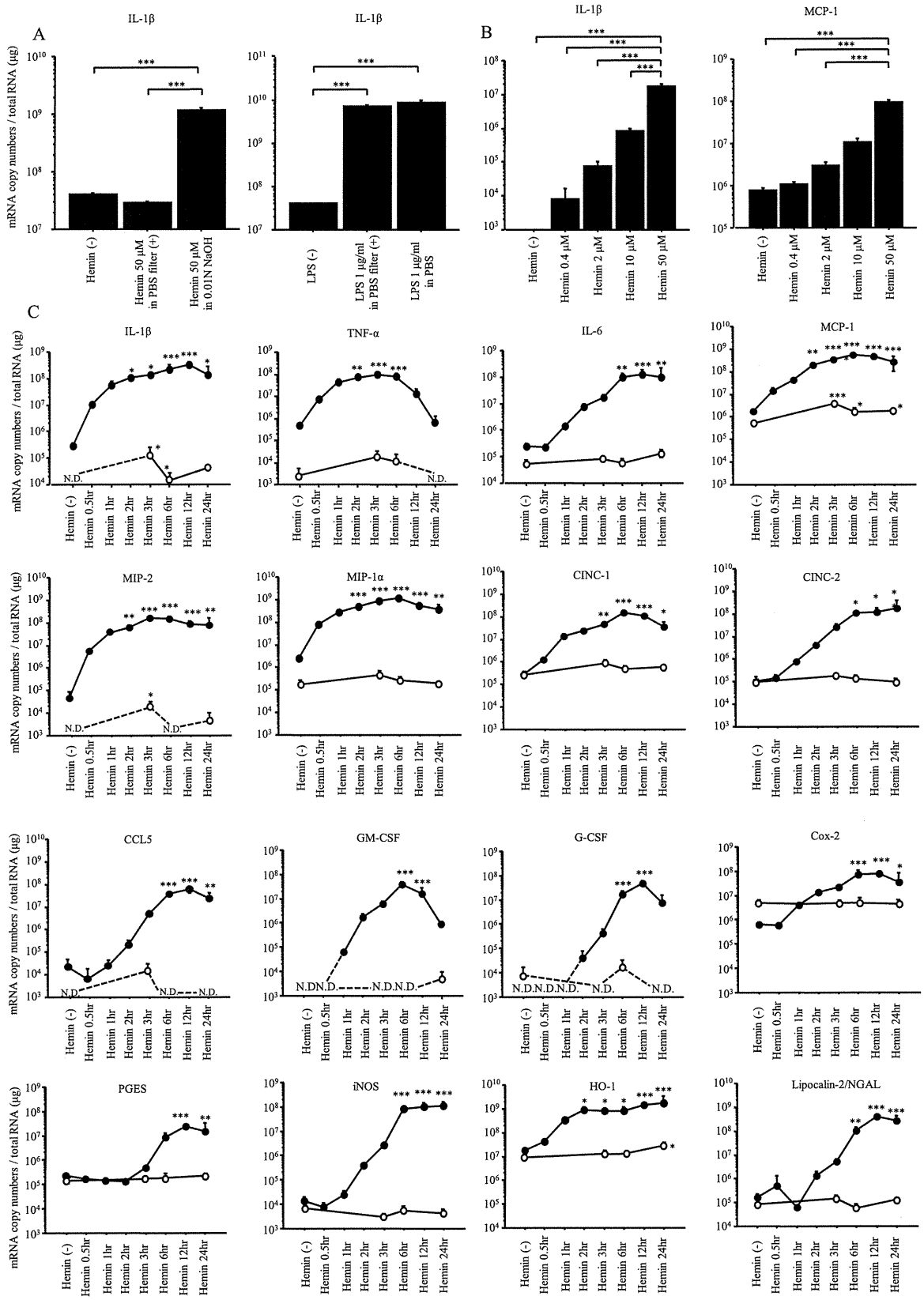

Fig. 3. IL-1β mRNAs in NR8383 stimulated with hemin and LPS in 0.01 N NaOH or PBS for 12 h (A). Hemin suspension and LPS solution in PBS were filtered with 0.22 μm filter. IL-1β and MCP-1 mRNAs in CCRC stimulated with serially diluting hemin for 24 h (B) and pro-inflammatory protein mRNAs and iron-related proteins in CCRC (closed circles) and CD11bc-negative CCRC (open circles) stimulated with 20 μM hemin (C). mRNAs were measured by quantitative RT-PCR. Results are representative of three independent experiments. Statistical assessment was performed by one-way ANOVA and Bonferroni's multiple comparison test. ***$P < 0.001$ vs hemin (−); **$P < 0.01$ vs hemin (−); *$P < 0.05$ vs hemin (−).

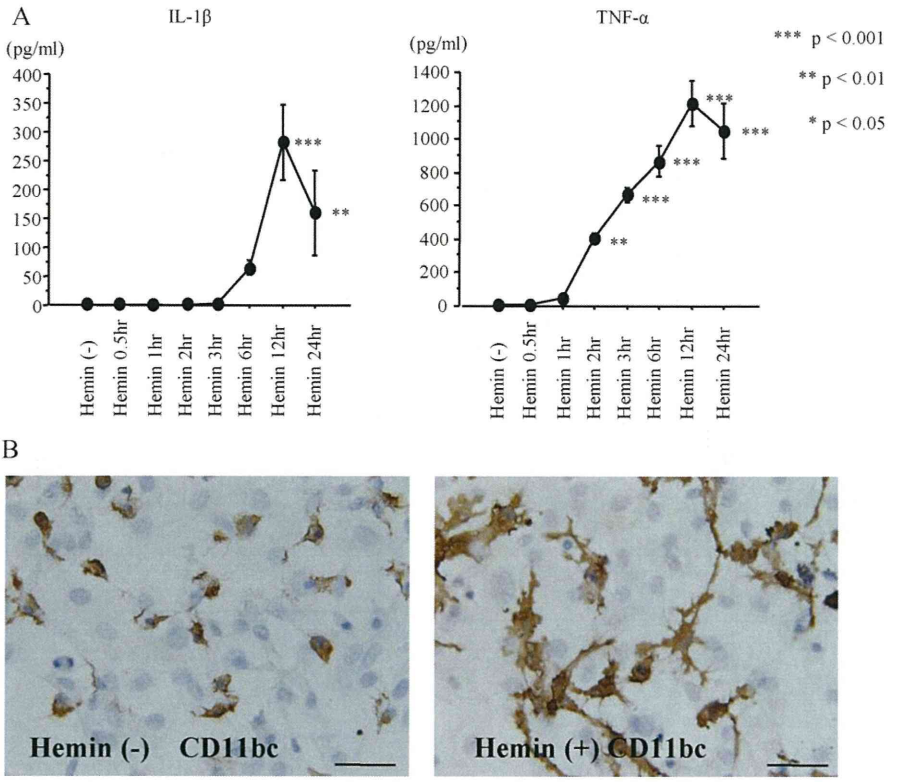

Fig. 4. IL-1β and TNF-α concentrations in CCRC culture medium (A) and alteration of CD11bc-positive cells morphology 24 h after hemin treatment (B). CCRC were stimulated with 20 μM hemin. Protein concentrations were measured by ELISA. Statistical assessment was performed by one-way ANOVA and Bonferroni's multiple comparison test. ***$P < 0.001$ vs hemin (−); **$P < 0.01$ vs hemin (−). Bar represents 50 μm.

leukemia virus reverse transcriptase. To create the plasmids used for the standard, mRNA of rat IL-1β, TNF-α, IL-6, MCP-1, macrophage inflammatory protein (MIP)-1α, MIP-2, cytokine-induced neutrophil chemoattractant (CINC)-1, CINC-2, chemokine (C–C motif) ligand 5 (CCL5), granulocyte colony-stimulating factor (G-CSF), granulocyte-macrophage colony-stimulating factor (GM-CSF), cyclooxygenase-2 (Cox-2), prostaglandin E synthase (PGES), inducible nitric oxide synthase (iNOS), HO-1 and Lcn2/NGAL were amplified from a rat experimental autoimmune myocarditis heart-derived cDNA library using the primer pairs (MIP-1α, sense primer 5′-ccttgctgttcttctctgcac-3′ and antisense primer 5′-catttagttccagctcagtgatgt-3′; CINC-1, sense primer 5′-acccgctcgcttctctgt-3′ and antisense primer 5′-cctttagcatcttttggacaatct-3′; CCL5, sense primer 5′-tgaagatctccacagctgcat-3′ and antisense primer 5′-attcttgaac-ccacttcttctctg-3′; G-CSF, sense primer 5′-cttaagtccttggagcaagtgag-3′ and antisense primer 5′-atccaggtgaagcatatccaag-3′; GM-CSF, sense primer 5′-atgtagatgccatcaaagaagctc-3′ and antisense primer 5′-ctttatgaaatcctcaaaggtggt-3′; HO-1, sense primer 5′-agtctatgcc-ccactctacttcc-3′ and antisense primer 5′-acgatagagctgtttgaacttggt-3′) and the primers as reported previously (Chang et al., 2006; Ding et al., 2010; Elnaggar et al., 2005; Liu et al., 2005; Yoshida et al., 2005). PCR-amplified cDNA inserts were directly inserted into the pGEM-T easy vector, and recombinant plasmids were isolated following transformation into *Escherichia coli* JM109-competent cells using a MagExtractor plasmid kit (Toyobo, Osaka, Japan). Absolute copy numbers of their mRNA were also measured by quantitative real-time RT-PCR using a LightCycler instrument together with the same primers and SYBR Premix Ex Taq (Takara, Otsu, Japan) used with our previously reported protocol (Chang et al., 2006). The absolute copy numbers of particular transcripts were calculated by LightCycler software using a standard curve approach.

2.6. Detection of IL-1β and TNF-α in culture medium

The concentrations of IL-1β and TNF-α in CCRC ($n = 4$) stimulated by hemin for 0.5, 1, 2, 3, 6, 12, and 24 h were measured using a rat IL-1β ELISA kit and a rat TNF-α ELISA Kit (R&D Systems).

2.7. Immunohistochemical staining of cultured cells and normal rat heart

For characterization of CCRC, the above-described CRC were cultured for 2 weeks on sterile Lab-Tek II chamber slides (Nalge Nunc International, Roskilde, Denmark) and were stimulated with 20 μM hemin for 24 h to examine alterations of cells morphology and frozen at −20 °C. The heart of a normal 8-week male Lewis rat was embedded in Tissue-Tek OCT compound (Miles Inc., Elkhart, IN) and frozen at −80 °C. Transverse sections 6 μm-thick were cut from the mid-ventricle slice with a cryostat. Slides were fixed with buffered methanol-acetone for 45 s and then placed in peroxidase-blocking solution (DakoCytomation, Vienna, Austria) for 30 min to block endogenous peroxidase activity. Slides were immunostained with mouse monoclonal α-smooth muscle actin Abs (Sigma–Aldrich), rabbit anti-factor VIII-related Ag Abs (Zymed Laboratories, South San Francisco, CA), rabbit anti-rat collagen type III Abs (Monosan, Uden, Netherlands), and mouse anti-rat CD11bc Abs (OX-42) (BD Pharmingen). The slides were washed in 0.05 M TBS three times. Immunodetection was performed using biotinylated anti-rabbit and anti-mouse Igs (LSAB2 kit; DakoCytomation) followed by horseradish peroxidase-conjugated

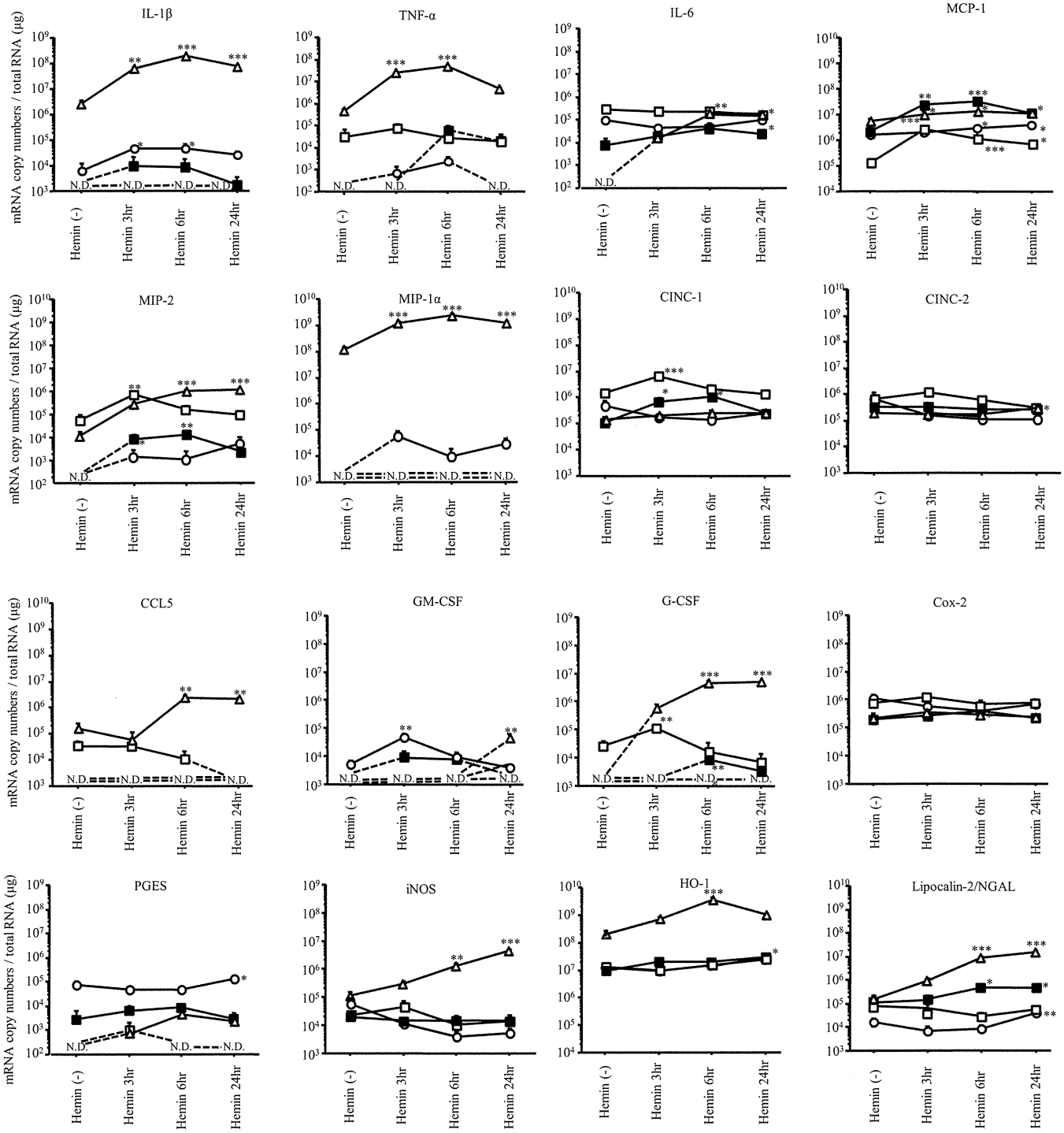

Fig. 5. Pro-inflammatory protein mRNAs and iron-related proteins in RCF (open circles), RASMC (closed squares), RHMVEC (open squares) and NR8383 (open triangles). Cultured cells were stimulated with 20 μM hemin and mRNAs were measured by quantitative RT-PCR. Results are representative of three independent experiments. Statistical assessment was performed by one-way ANOVA and Bonferroni's multiple comparison test. ***$P < 0.001$ vs hemin (−); **$P < 0.01$ vs hemin (−); *$P < 0.05$ vs hemin (−).

streptavidin and 3,3′-diaminobenzidine (DAB) substrate (Dako-Cytomation). The sections were lightly counterstained with Mayer's hematoxylin. Negative control slides were incubated with either mouse IgG2a or normal rabbit serum instead of the primary Ab. Cytospin preparations of CD11bc-positive CRC and the slides containing CCRC were also stained with May-Grunwald/Giemsa.

2.8. ROS detection by flow cytometry

Intracellular ROS levels in CCRC were measured by the CM-H2DCFDA assay using 5-(and-6)-chloromethyl-2′,7′-dichlorodihydrofluorescein diacetate, acetyl-ester (Molecular Probes, Eugene, OR). These analyses were performed four times independently. CCRC were maintained in the above-described

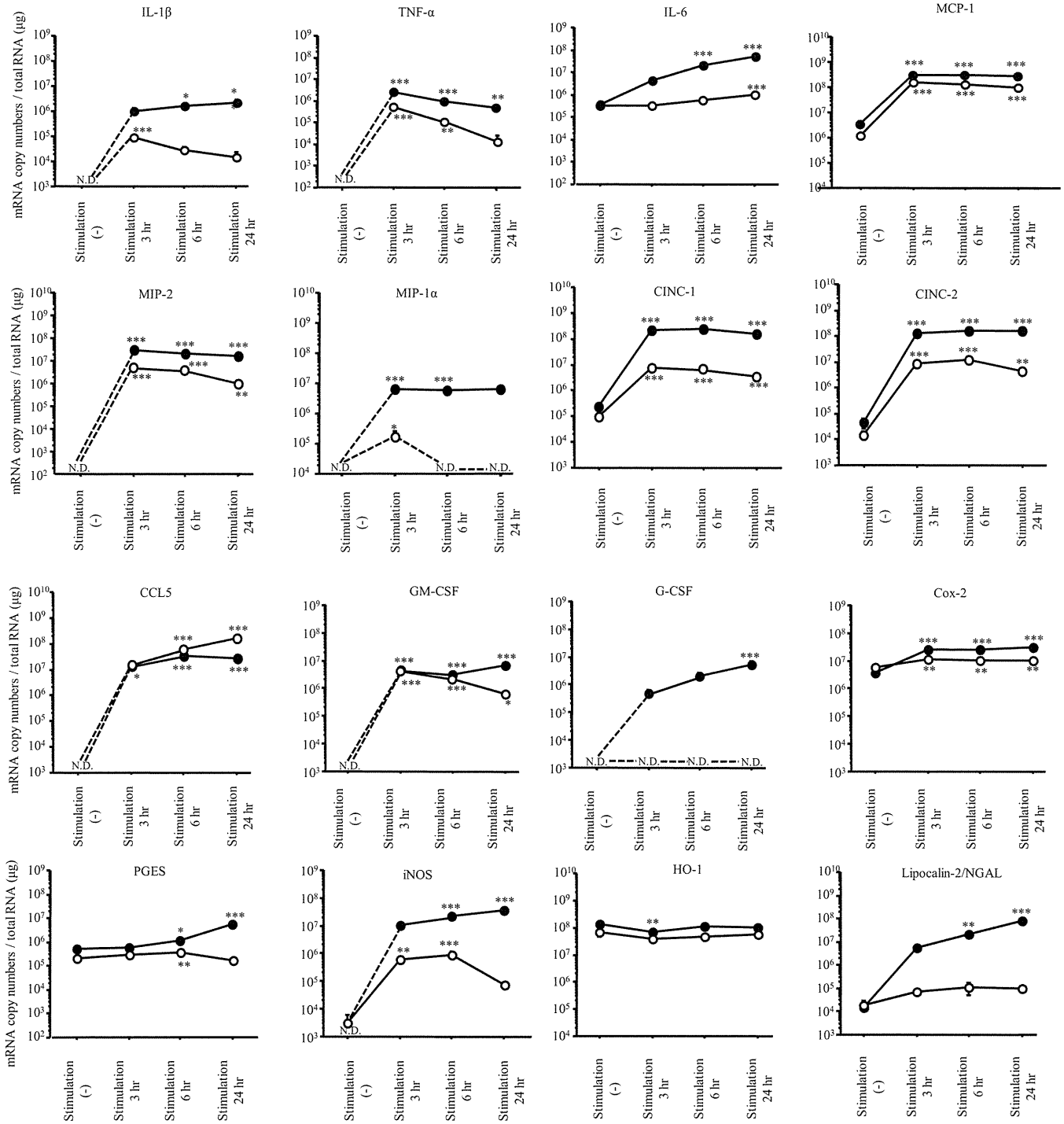

Fig. 6. Pro-inflammatory protein mRNAs and iron-related proteins in CD11bc-negative CCRC. Cultured cells of CD11bc-negative CRC were stimulated with 2.5 ng/ml IL-1α (closed circles) and 10 ng/ml TNF-α (open circles) and mRNAs were measured by quantitative RT-PCR. Statistical assessment was performed by one-way ANOVA and Bonferroni's multiple comparison test. ***$P < 0.001$ vs stimulation (−); **$P < 0.01$ vs stimulation (−); *$P < 0.05$ vs stimulation (−).

media until 80–90% confluent, switched to 1 ml phosphate buffered saline (PBS) with CM-H2DCFDA and treated with hemin for 1 h. CCRC were washed in PBS and detached by changing to 2 ml 0.25% trypsin–EDTA. CCRC were suspended in PBS with 0.002% trypan blue and analyzed using a FACScan flow cytometer. To inhibit ROS production, Tiron (4,5-dihydroxy-1,3-benzenedisulfonic acid) (Sigma–Aldrich) was added 3 h before hemin stimulation and was also added in PBS with CM-H2DCFDA.

2.9. Quantification of NF-κB activation

NR8383 ($n = 4$) were stimulated with 20 μM hemin for 1 h and nuclear protein fractions were prepared using the Nuclear Extract

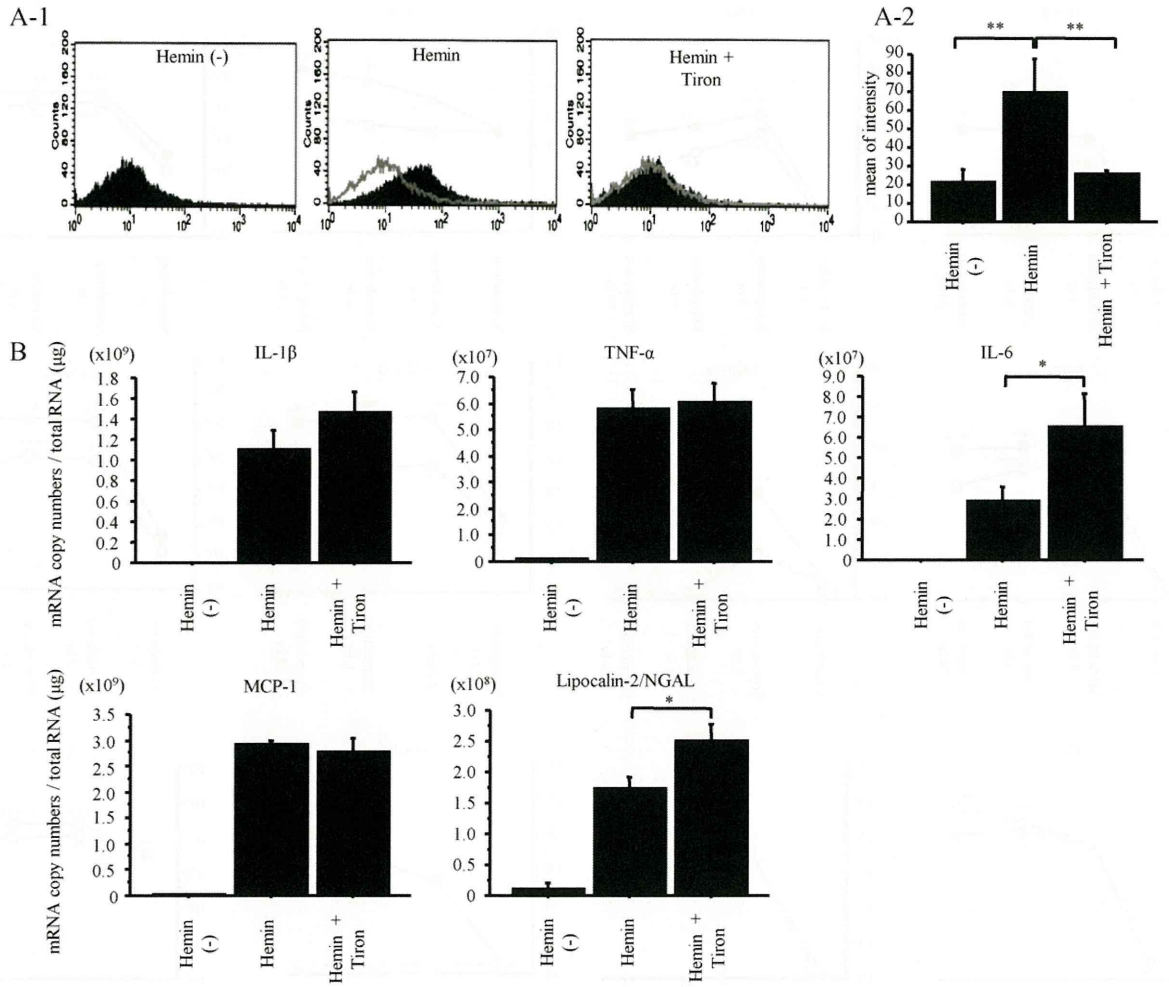

Fig. 7. Intracellular ROS levels (A-1 and A-2) and mRNAs of pro-inflammatory proteins and lipocalin-2/NGAL (B) in CCRC. (A) Intracellular ROS levels in CCRC were measured by flow cytometry. CCRC in PBS with CM-H2DCFDA were stimulated with hemin for 1 h. 10 mM Tiron was added 3 h before hemin stimulation. Flow cytometry results shown (A-1) are representative of four independent experiments. Mean fluorescence intensities (A-2) were analyzed from four experiments. Statistical assessment was performed by one-way ANOVA and Bonferroni's multiple comparison test. $^{**}P < 0.01$. (B) mRNAs were measured by quantitative RT-PCR. CCRC were stimulated with 20 μM hemin in RPMI medium containing 10% FBS and 10 mM Tiron was added 3 h before hemin stimulation. These analyses are representative of three independent experiments. Statistical assessment was performed by one-way ANOVA and Bonferroni's multiple comparison test. $^{*}P < 0.05$ vs hemin (+).

Kit (Active Motif, Carlsbad, CA). The activity of NF-κB subunit p65 was determined with the Trans-AM NF-κB ELISA kit and Recombinant NFκB p65 protein (Active Motif).

2.10. Statistical analysis

Statistical assessment was performed by one-way ANOVA and Bonferroni's multiple comparison test or non-paired Student's *t*-test. Differences were considered significant at $P < 0.05$. Data obtained from quantitative RT-PCR, ELISA and mean fluorescence intensity were expressed as the mean ± SEM.

3. Results

3.1. Characterization of cardiac resident cells and CCRC

Immunohistochemistry of CCRC showed that most cells were α-smooth muscle actin- and collagen type III-positive, which were concluded to be smooth muscle cells or fibroblasts; some were CD11bc-positive cells, which were concluded to be macrophages; however there were no cardiomyocytes and no factor VIII-related Ag-positive cells which would have indicated the presence of endothelial cells (Fig. 1A–E). Flow cytometry of CCRC demonstrated that approximately 10–15% were CD11bc-positive, 1% were RT1B (MHC class II)-positive and 80–90% were all-negative cells, which were concluded to be smooth muscle cells or fibroblasts (Fig. 1H). Flow cytometry of CRC immediately before culture demonstrated that approximately 10% were CD11bc-positive cells, which were almost completely removed after sorting (Fig. 2A). Most of the CD11bc-positive cells were neutrophils and macrophages, but after culture, neutrophils disappeared and only mononuclear cells thought to be macrophages remained (Figs. 1B and 2A). Immunohistochemical staining of normal rat heart showed that CD11bc-positive cells concluded to be cardiac resident macrophages were broadly distributed (Fig. 2B).

3.2. Change of gene expression, protein production and alterations of morphology by hemin in cultured cells

First, we ruled out possible LPS contamination by two methods that make use of the different solubilities of hemin and LPS in phosphate-buffered saline (PBS). Hemin seems to be soluble not in PBS but in water with NaOH. On the other hand, LPS seems to be soluble also in PBS. In the first method, we used Endotoxin Detection System (GenScript USA Inc., Piscataway, NJ) measuring with a spectrophotometer and did not detect LPS endotoxin contamina-

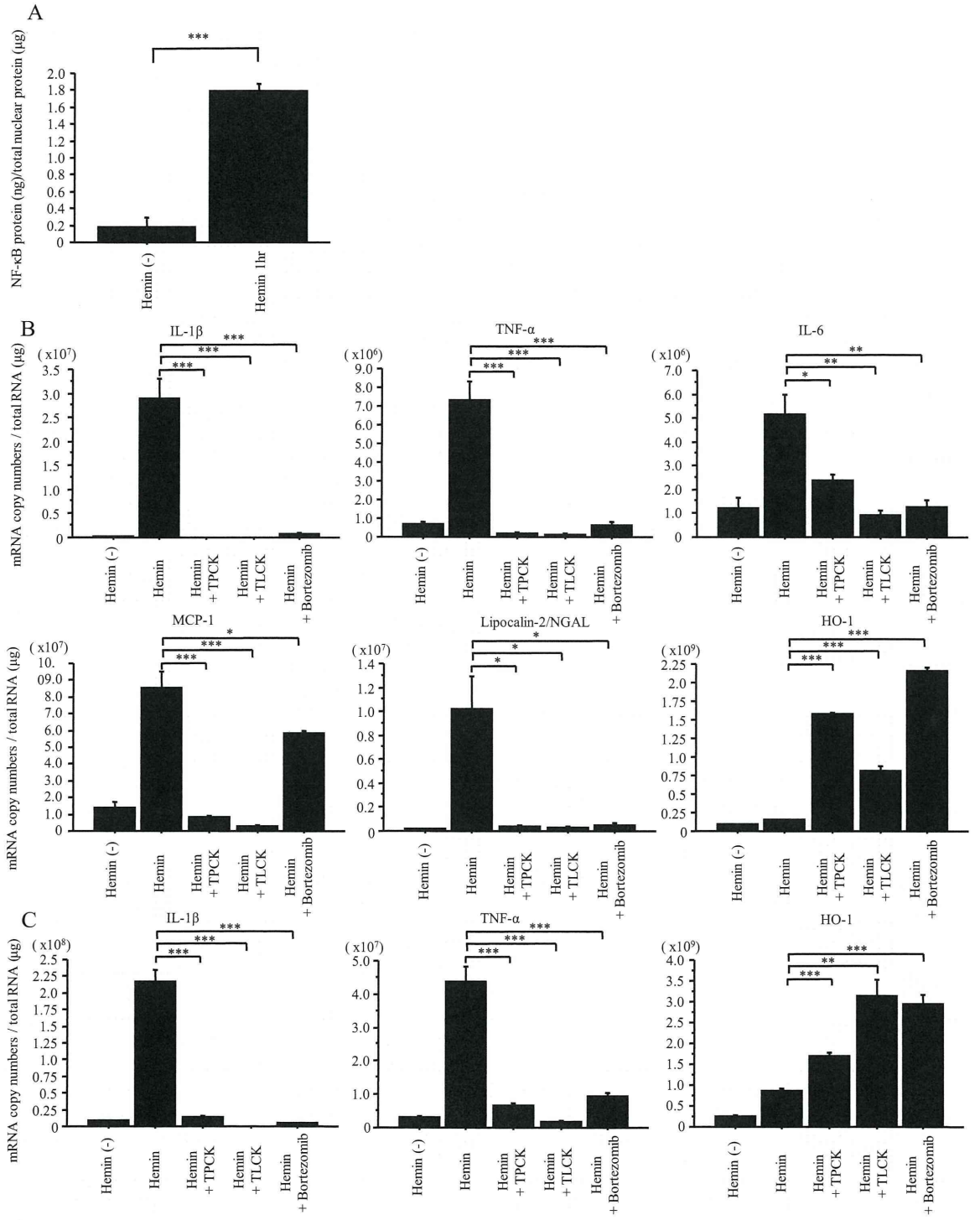

Fig. 8. NF-κB activation, pro-inflammatory protein mRNAs and iron-related proteins in NR8383 and CCRC. (A) NF-κB activation in NR8383 was measured by ELISA. NR8383 were stimulated with 20 μM hemin for 1 h. Statistical assessment was performed by non-paired Student's *t*-test. ***$P < 0.001$. (B) mRNAs in CCRC were measured by quantitative RT-PCR. (C) mRNAs in NR8383 were measured by quantitative RT-PCR. CCRC (B) and NR8383 (C) were stimulated with 20 μM hemin. 25 μM TPCK, 300 μM TLCK and 10 μM Bortezomib were added 1 h before hemin stimulation. These analyses (B and C) are representative of three independent experiments. Statistical assessment was performed by one-way ANOVA and Bonferroni's multiple comparison test. ***$P < 0.001$ vs hemin (+); **$P < 0.01$ vs hemin (+); *$P < 0.05$ vs hemin (+).

tion in the hemin-free and colorless filtrate that was obtained by passing hemin suspension in PBS through 0.22 μm filter (Millipore, Billerica, MA) (data not shown). In the other method, we examined induction of IL-1 in NR8383 by previously described hemin-free filtrate. IL-1 expression in NR8383 was markedly induced not by hemin-free filtrate but by hemin solution in NaOH (Fig. 3A). Because LPS is soluble in PBS, LPS in PBS must pass through 0.22 μm filter. In fact, we found that IL-1 expression was markedly induced by LPS in PBS passed through 0.22 μm filter as well as by that before filtration (Fig. 3A). These findings indicate no LPS contamination in hemin.

Next, we examined induction of various gene expressions by hemin. Surprisingly, hemin induced IL-1β and MCP-1 mRNA expression in a dose-dependent manner (Fig. 3B) and marked mRNA expression of various pro-inflammatory proteins in CCRC (Fig. 3C). In all cases mRNA expression was increased by at least

100-fold within 24 h after addition of hemin. Protein levels of IL-1β and TNF-α in CCRC culture medium also markedly increased after addition of hemin (Fig. 4A). Treatment with hemin dramatically altered the morphology of CD11bc-positive cells. Almost all CD11bc-positive cells became activated macrophage that were characterized by an increase in size, and changes of shape (Fig. 4B). Gene expression of iron metabolism-related proteins such as HO-1 and Lcn2/NGAL also greatly increased, by at least 100-fold (Fig. 3C). However, in the case of CD11bc-negative CCRC, RASMC, RHMVEC and RCF, expression of only a few pro-inflammatory and iron-related proteins slightly increased after hemin stimulation and in most cases there was no increase (Figs. 3C and 5). On the other hand, expression of IL-1β, TNF-α, MIP-1α, MIP-2, G-CSF, iNOS, HO-1 and Lcn/NGAL strongly increased in NR8383 (Fig. 5), while expression levels of some other proteins such as CINC-1,CINC-2, Cox-2, and PGES did not increase or only slightly increased, unlike the effects seen in CCRC (Figs. 3C and 5).

3.3. Change of gene expression by IL-1 and TNF-α in CD11bc-negative CCRC

Expression of pro-inflammatory and iron-related proteins in CD11bc-negative CCRC did not increase after hemin stimulation (Fig. 3C); however, on IL-1α- or TNF-α-stimulation, expression of most of these proteins was strongly increased to a similar extent as in CCRC after addition of hemin (Fig. 6).

3.4. Intracellular ROS production and NF-κB activation by hemin and effect of inhibitors of ROS and NF-κB

Intracellular ROS production in CCRC was significantly induced by hemin stimulation (Fig. 7A). The superoxide scavenger Tiron almost completely suppressed the induction of intracellular ROS (Fig. 7A). However, Tiron did not suppress expression of pro-inflammatory proteins and iron-related proteins in CCRC stimulated with hemin (Fig. 7B). NF-κB activation in NR8383 was significantly induced by hemin stimulation (Fig. 8A). TPCK, TLCK and Bortezomib, which were proteasome inhibitors and therefore also acted as NF-κB inhibitors, strongly suppressed expression of most pro-inflammatory proteins in CCRC; in contrast however, expression of HO-1 was increased (Fig. 8B). These findings were also observed in NR8383 (Fig. 8C).

4. Discussion

Several novel findings emerged from this study. First, hemin induced various pro-inflammatory proteins also in CCRC, which were cultured in ordinary medium, though free iron did not induce them (data not shown). Hemin itself is thought to induce them because we ruled out LPS contamination as described above (Fig. 3A) and bacterial contamination by microscopic observations. Second, hemin-targeted cells were mainly cultured cardiac resident macrophages. They were also morphologically altered by hemin stimulation. Third, IL-1 and TNF-α induced various pro-inflammatory proteins in cardiac resident smooth muscle cells, fibroblasts, etc. Our study didn't find that IL-6 induced expression of proinflammatory proteins such as MCP-1 et al. (data not shown). In particular, IL-1 and TNF-α are considered to be important cytokines because they are widely known to induce many other pro-inflammatory proteins (Dinarello, 1991; Wallach et al., 1999). IL-1 and TNF-α are thought to be produced by macrophages which are hemin-targeted cells. The macrophage cell line NR8383, as well as CCRC containing CD11bc-positive cells (cardiac resident macrophages) also increased expression of IL-1β and TNF-α on hemin stimulation; however, CD11bc-negative CCRC did not. Our previous studies demonstrated that IL-1 and TNF-α producing cells in rat autoimmune myocarditis were almost all CD11bc-positive cells (Liu et al., 2005; Yoshida et al., 2005). On the other hand, CD11bc-negative CCRC increased expression of various pro-inflammatory proteins via IL-1 or TNF-α stimulation but not via hemin stimulation. These findings indicated that CD11bc-positive CCRC stimulated by hemin produced IL-1, TNF-α, etc. while CD11bc-negative CCRC enhanced production of various pro-inflammatory proteins via IL-1- and TNF-α stimulation.

The existence of cardiac resident macrophages was reported almost twenty years ago (Smith and Allen, 1992; Spencer and Fabre, 1990), but little is known about their role. The results of our immunohistochemical and flow cytometric analyses showed that CD11bc-positive cells (cardiac resident macrophages) were widely distributed in normal rat hearts. Cardiac resident macrophages may be a key cell type in the pathogenesis of cardiac inflammation and remodeling. Tissue-resident macrophages are thought to constitute 10–15% of most tissues (Medzhitov, 2008). Recent studies have revealed that Kupffer cells (Seki and Brenner, 2008), Langerhans cells (Berger et al., 2006), and microglia (Block et al., 2007), which are tissue resident macrophages, react to damage-associated molecular patterns (Medzhitov, 2008; Zitvogel et al., 2010), and their importance in tissue injury has been emphasized. Microglia have been implicated as active contributors to neuron damage in various neurodegenerative diseases (Block et al., 2007). Further studies are needed to assess the role of cardiac resident macrophages in various heart diseases such as myocardial infarction, myocarditis and cardiomyopathy. Moreover, CD11bc-negative cells (cardiac smooth muscle cells, fibroblasts, etc.) are suggested to play an important role in enhancing inflammation. Our previous study of rat autoimmune myocarditis demonstrated that MCP-1, IL-6, Cox-2, PGES, and CINC-2 were mainly expressed in these cells rather than in CD11bc-positive cells (Chang et al., 2006; Yoshida et al., 2005). Though cardiac smooth muscle cells and fibroblasts have generally been considered to be important for cardiac repair (Frangogiannis, 2008; Porter and Turner, 2009), our studies suggested that these cells initially promote inflammation and injury in hearts and may be supporting players in inflammation via cross-talk with resident macrophages.

Our recent studies have demonstrated that expression of iron-related proteins strongly increases in myocarditis and myocardial infarction (Ding et al., 2010; Isoda et al., 2010; Watanabe et al., 2008) and these results have provided the motivation for the present study. In fact, free heme strongly induced expression of HO-1 and Lcn/NGAL in CCRC. Although it is well known that hemin induces HO-1 expression (Kanakiriya et al., 2003; Tsiftsoglou et al., 2006), the induction of Lcn/NGAL by hemin stimulation has not been previously reported. Expression of Lcn2/NGAL has been reported to be induced by IL-1 (Cowland et al., 2003; Yndestad et al., 2009). Our present study demonstrated that Lcn2/NGAL expression in CD11bc-negative CCRC was induced not by hemin but by IL-1. The induction of Lcn/NGAL in this study is thought to be due to the production of IL-1 by hemin stimulation in CD11bc-positive cells. Lcn2/NGAL transports extracelluar iron into cells or exports intracellular iron from cells. Large amounts of hemin in injured hearts induce HO-1 production and are catabolized by HO-1; thus iron is thought to accumulate in such hearts. Lcn2/NGAL may transport extracellular iron into macrophages, fibroblasts, smooth muscle cells, etc. Since extracellular iron seems to generate ROS (Halliwell and Gutteridge, 1992), Lcn2/NGAL may suppress ROS production and reduce cardiac injury by storage of iron in ferritin (Balla et al., 1992).

For the first time, we have investigated whether the induction of pro-inflammatory proteins by hemin stimulation was dependent on the production of ROS. This was because there have been some reports of upregulation of Egr-1 and IL-8 expression via ROS (Hasan and Schafer, 2008; Natarajan et al., 2007); it has also been pro-

posed that ROS may be important for inflammasome activation, which is involved in processing and secretion of IL-1β (Church et al., 2008; Cruz et al., 2007; Dostert et al., 2008) However, the results of the present study did not suggest that increase of pro-inflammatory protein expression was dependent on ROS. On the other hand, hemin induced NF-κB activation, while protease and proteasome inhibitors strongly suppressed the induction of pro-inflammatory protein expression. This suppression by protease and proteasome inhibitors, which inhibit IκB degradation, suggests that hemin induces expression of pro-inflammatory proteins via NF-κB activation. In one report, free heme induced TNF-α secretion by macrophages in a TLR4-dependent manner (Figueiredo et al., 2007). The TLR4 ligand LPS produces large amounts of pro-inflammatory cytokines such as IL-1 and TNF-α (Eskay et al., 1990). and it is well known that signaling by LPS, IL-1 and TNF-α induces NF-κB activation by the degradation of IκB in proteasomes (Baldwin, 1996). On the other hand, the present study showed that protease and proteasome inhibitors enhanced hemin-induced HO-1 expression, in contrast to expressed pro-inflammatory proteins. Some previous studies reported that the protease inhibitor MG-132 increased HO-1 expression and that the mechanism depends on inhibition of degradation of Nrf2, a stress-responsive transcription factor (Chen and Regan, 2005; Dreger et al., 2009). Our results agree with these previous studies. The induction of expression of various genes by free heme seems to be caused by a number of different signaling pathways.

Our study has shown that free heme, a stimulator of ROS production, strongly induced expression of pro-inflammatory proteins and the antioxidant defense enzyme HO-1 in CCRC. Since large amounts of heme proteins are contained in cardiomyocytes and since, in the case of cardiac injury, free heme is generated in such cells, further studies are needed to clarify the influence of free heme on cardiac resident cells as an important contribution to our understanding of cardiac injury and cardiac remodeling.

Acknowledgements

This study was supported in part by a Ministry of Health, Labor, and Welfare in Japan grant "Research on Regulatory Science of Pharmaceutical and Medical Devices" and by a grant for scientific research from the Ministry of Education, Science and Culture of Japan (number 20591185)

References

Allen, I.C., Scull, M.A., Moore, C.B., Holl, E.K., McElvania-TeKippe, E., Taxman, D.J., Guthrie, E.H., Pickles, R.J., Ting, J.P., 2009. The NLRP3 inflammasome mediates in vivo innate immunity to influenza a virus through recognition of viral RNA. Immunity 30, 556–565.

Baldwin Jr., A.S., 1996. The NF-kappa B and I kappa B proteins: new discoveries and insights. Annu. Rev. Immunol. 14, 649–683.

Balla, G., Jacob, H.S., Balla, J., Rosenberg, M., Nath, K., Apple, F., Eaton, J.W., Vercellotti, G.M., 1992. Ferritin: a cytoprotective antioxidant strategem of endothelium. J. Biol. Chem. 267, 18148–18153.

Berger, C.L., Vasquez, J.G., Shofner, J., Mariwalla, K., Edelson, R.L., 2006. Langerhans cells: mediators of immunity and tolerance. Int. J. Biochem. Cell Biol. 38, 1632–1636.

Beri, R., Chandra, R., 1993. Chemistry and biology of heme. Effect of metal salts, organometals, and metalloporphyrins on heme synthesis and catabolism, with special reference to clinical implications and interactions with cytochrome P-450. Drug Metab. Rev. 25, 149–152.

Block, M.L., Zecca, L., Hong, J.S., 2007. Microglia-mediated neurotoxicity: uncovering the molecular mechanisms. Nat. Rev. Neurosci. 8, 57–69.

Brown, D.A., MacLellan, W.R., Laks, H., Dunn, J.C., Wu, B.M., Beygui, R.E., 2007. Analysis of oxygen transport in a diffusion-limited model of engineered heart tissue. Biotechnol. Bioeng. 97, 962–975.

Chang, H., Hanawa, H., Liu, H., Yoshida, T., Hayashi, M., Watanabe, R., Abe, S., Toba, K., Yoshida, K., Elnaggar, R., Minagawa, S., Okura, Y., Kato, K., Kodama, M., Maruyama, H., Miyazaki, J., Aizawa, Y., 2006. Hydrodynamic-based delivery of an interleukin-22-Ig fusion gene ameliorates experimental autoimmune myocarditis in rats. J. Immunol. 177, 3635–3643.

Chen, J., Regan, R.F., 2005. Increasing expression of heme oxygenase-1 by proteasome inhibition protects astrocytes from heme-mediated oxidative injury. Curr. Neurovasc. Res. 2, 189–196.

Chen, W., Syldath, U., Bellmann, K., Burkart, V., Kolb, H., 1999. Human 60-kDa heat-shock protein: a danger signal to the innate immune system. J. Immunol. 162, 3212–3219.

Church, L.D., Cook, G.P., McDermott, M.F., 2008. Primer: inflammasomes and interleukin 1beta in inflammatory disorders. Nat. Clin. Pract. Rheumatol. 4, 34–42.

Cowland, J.B., Sorensen, O.E., Sehested, M., Borregaard, N., 2003. Neutrophil gelatinase-associated lipocalin is up-regulated in human epithelial cells by IL-1 beta, but not by TNF-alpha. J. Immunol. 171, 6630–6639.

Cruz, C.M., Rinna, A., Forman, H.J., Ventura, A.L., Persechini, P.M., Ojcius, D.M., 2007. ATP activates a reactive oxygen species-dependent oxidative stress response and secretion of proinflammatory cytokines in macrophages. J. Biol. Chem. 282, 2871–2879.

Dinarello, C.A., 1991. Interleukin-1 and interleukin-1 antagonism. Blood 77, 1627–1652.

Ding, L., Hanawa, H., Ota, Y., Hasegawa, G., Hao, K., Asami, F., Watanabe, R., Yoshida, T., Toba, K., Yoshida, K., Ogura, M., Kodama, M., Aizawa, Y., 2010. Lipocalin-2/neutrophil gelatinase-B associated lipocalin is strongly induced in hearts of rats with autoimmune myocarditis and in human myocarditis. Circ. J. 74, 523–530.

Dostert, C., Petrilli, V., Van Bruggen, R., Steele, C., Mossman, B.T., Tschopp, J., 2008. Innate immune activation through Nalp3 inflammasome sensing of asbestos and silica. Science 320, 674–677.

Dreger, H., Westphal, K., Weller, A., Baumann, G., Stangl, V., Meiners, S., Stangl, K., 2009. Nrf2-dependent upregulation of antioxidative enzymes: a novel pathway for proteasome inhibitor-mediated cardioprotection. Cardiovasc. Res. 83, 354–361.

Eghbali, M., Czaja, M.J., Zeydel, M., Weiner, F.R., Zern, M.A., Seifter, S., Blumenfeld, O.O., 1988. Collagen chain mRNAs in isolated heart cells from young and adult rats. J. Mol. Cell. Cardiol. 20, 267–276.

Elnaggar, R., Hanawa, H., Liu, H., Yoshida, T., Hayashi, M., Watanabe, R., Abe, S., Toba, K., Yoshida, K., Chang, H., Minagawa, S., Okura, Y., Kato, K., Kodama, M., Maruyama, H., Miyazaki, J., Aizawa, Y., 2005. The effect of hydrodynamics-based delivery of an IL-13-Ig fusion gene for experimental autoimmune myocarditis in rats and its possible mechanism. Eur. J. Immunol. 35, 1995–2005.

Eskay, R.L., Grino, M., Chen, H.T., 1990. Interleukins, signal transduction, and the immune system-mediated stress response. Adv. Exp. Med. Biol. 274, 331–343.

Figueiredo, R.T., Fernandez, P.L., Mourao-Sa, D.S., Porto, B.N., Dutra, F.F., Alves, L.S., Oliveira, M.F., Oliveira, P.L., Graca-Souza, A.V., Bozza, M.T., 2007. Characterization of heme as activator of Toll-like receptor 4. J. Biol. Chem. 282, 20221–20229.

Frangogiannis, N.G., 2008. The immune system and cardiac repair. Pharmacol. Res. 58, 88–111.

Frantz, S., Ertl, G., Bauersachs, J., 2007. Mechanisms of disease: Toll-like receptors in cardiovascular disease. Nat. Clin. Pract. Cardiovasc. Med. 4, 444–454.

Halliwell, B., Gutteridge, J.M., 1992. Biologically relevant metal ion-dependent hydroxyl radical generation. An update. FEBS Lett. 307, 108–112.

Hasan, R.N., Schafer, A.I., 2008. Hemin upregulates Egr-1 expression in vascular smooth muscle cells via reactive oxygen species ERK-1/2-Elk-1 and NF-kappaB. Circ. Res. 102, 42–50.

Isoda, M., Hanawa, H., Watanabe, R., Yoshida, T., Toba, K., Yoshida, K., Kojima, M., Otaki, K., Hao, K., Ding, L., Tanaka, K., Takayama, T., Kato, K., Okura, O., Kodama, M., Ota, Y., Hayashi, J., Aizawa, Y., 2010. Expression of the peptide hormone hepcidin increases in cardiomyocytes under myocarditis and myocardial infarction. J. Nutr. Biochem. 21, 749–756.

Kanakiriya, S.K., Croatt, A.J., Haggard, J.J., Ingelfinger, J.R., Tang, S.S., Alam, J., Nath, K.A., 2003. Heme: a novel inducer of MCP-1 through HO-dependent and HO-independent mechanisms. Am. J. Physiol. Renal Physiol. 284, F546–F554.

Liu, H., Hanawa, H., Yoshida, T., Elnaggar, R., Hayashi, M., Watanabe, R., Toba, K., Yoshida, K., Chang, H., Okura, Y., Kato, K., Kodama, M., Maruyama, H., Miyazaki, J., Nakazawa, M., Aizawa, Y., 2005. Effect of hydrodynamics-based gene delivery of plasmid DNA encoding interleukin-1 receptor antagonist-Ig for treatment of rat autoimmune myocarditis: possible mechanism for lymphocytes and noncardiac cells. Circulation 111, 1593–1600.

Medzhitov, R., 2008. Origin and physiological roles of inflammation. Nature 454, 428–435.

Nakahira, K., Takahashi, T., Shimizu, H., Maeshima, K., Uehara, K., Fujii, H., Nakatsuka, H., Yokoyama, M., Akagi, R., Morita, K., 2003. Protective role of heme oxygenase-1 induction in carbon tetrachloride-induced hepatotoxicity. Biochem. Pharmacol. 66, 1091–1105.

Natarajan, R., Fisher, B.J., Fowler 3rd, A.A., 2007. Hypoxia inducible factor-1 modulates hemin-induced IL-8 secretion in microvascular endothelium. Microvasc. Res. 73, 163–172.

Okamura, Y., Watari, M., Jerud, E.S., Young, D.W., Ishizaka, S.T., Rose, J., Chow, J.C., Strauss 3rd, J.F., 2001. The extra domain A of fibronectin activates Toll-like receptor 4. J. Biol. Chem. 276, 10229–10233.

Porter, K.E., Turner, N.A., 2009. Cardiac fibroblasts: at the heart of myocardial remodeling. Pharmacol. Ther. 123, 255–278.

Scheibner, K.A., Lutz, M.A., Boodoo, S., Fenton, M.J., Powell, J.D., Horton, M.R., 2006. Hyaluronan fragments act as an endogenous danger signal by engaging TLR2. J. Immunol. 177, 1272–1281.

Seki, E., Brenner, D.A., 2008. Toll-like receptors and adaptor molecules in liver disease: update. Hepatology 48, 322–335.

Shi, Y., Evans, J.E., Rock, K.L., 2003. Molecular identification of a danger signal that alerts the immune system to dying cells. Nature 425, 516–521.
Smith, S.C., Allen, P.M., 1992. Expression of myosin-class II major histocompatibility complexes in the normal myocardium occurs before induction of autoimmune myocarditis. Proc. Natl. Acad. Sci. U. S. A. 89, 9131–9135.
Spencer, S.C., Fabre, J.W., 1990. Characterization of the tissue macrophage and the interstitial dendritic cell as distinct leukocytes normally resident in the connective tissue of rat heart. J. Exp. Med. 171, 1841–1851.
Stone, M.J., Willerson, J.T., Gomez-Sanchez, C.E., Waterman, M.R., 1975. Radioimmunoassay of myoglobin in human serum. Results in patients with acute myocardial infarction. J. Clin. Invest. 56, 1334–1339.
Trendelenburg, G., 2008. Acute neurodegeneration and the inflammasome: central processor for danger signals and the inflammatory response? J. Cereb. Blood Flow Metab. 28, 867–881.
Tsiftsoglou, A.S., Tsamadou, A.I., Papadopoulou, L.C., 2006. Heme as key regulator of major mammalian cellular functions: molecular, cellular, and pharmacological aspects. Pharmacol. Ther. 111, 327–345.
Wagener, Feldman, E., de Witte, T., Abraham, N.G., 1997. Heme induces the expression of adhesion molecules ICAM-1, VCAM-1, and E selectin in vascular endothelial cells. Proc. Soc. Exp. Biol. Med. 216, 456–463.
Wagener, F.A., Eggert, A., Boerman, O.C., Oyen, W.J., Verhofstad, A., Abraham, N.G., Adema, G., van Kooyk, Y., de Witte, T., Figdor, C.G., 2001. Heme is a potent inducer of inflammation in mice and is counteracted by heme oxygenase. Blood 98, 1802–1811.
Wallach, D., Varfolomeev, E.E., Malinin, N.L., Goltsev, Y.V., Kovalenko, A.V., Boldin, M.P., 1999. Tumor necrosis factor receptor and Fas signaling mechanisms. Annu. Rev. Immunol. 17, 331–367.
Watanabe, R., Hanawa, H., Yoshida, T., Ito, M., Isoda, M., Chang, H., Toba, K., Yoshida, K., Kojima, M., Otaki, K., Ding, L., Hao, K., Kato, K., Kodama, M., Aizawa, Y., 2008. Gene expression profiles of cardiomyocytes in rat autoimmune myocarditis by DNA microarray and increase of regenerating gene family. Transl. Res. 152, 119–127.
Wittenberg, B.A., Wittenberg, J.B., 1987. Myoglobin-mediated oxygen delivery to mitochondria of isolated cardiac myocytes. Proc. Natl. Acad. Sci. U. S. A. 84, 7503–7507.
Wittenberg, J.B., Wittenberg, B.A., 2003. Myoglobin function reassessed. J. Exp. Biol. 206, 2011–2020.
Yndestad, A., Landro, L., Ueland, T., Dahl, C.P., Flo, T.H., Vinge, L.E., Espevik, T., Froland, S.S., Husberg, C., Christensen, G., Dickstein, K., Kjekshus, J., Oie, E., Gullestad, L., Aukrust, P., 2009. Increased systemic and myocardial expression of neutrophil gelatinase-associated lipocalin in clinical and experimental heart failure. Eur. Heart J. 30, 1229–1236.
Yoshida, T., Hanawa, H., Toba, K., Watanabe, H., Watanabe, R., Yoshida, K., Abe, S., Kato, K., Kodama, M., Aizawa, Y., 2005. Expression of immunological molecules by cardiomyocytes and inflammatory and interstitial cells in rat autoimmune myocarditis. Cardiovasc. Res. 68, 278–288.
Zak, R., 1973. Cell proliferation during cardiac growth. Am. J. Cardiol. 31, 211–219.
Zitvogel, L., Kepp, O., Kroemer, G., 2010. Decoding cell death signals in inflammation and immunity. Cell 140, 798–804.

Inflamm. Res.
DOI 10.1007/s00011-011-0401-y

Inflammation Research

ORIGINAL RESEARCH PAPER

Severe neutrophil-mediated lung inflammation in myeloperoxidase-deficient mice exposed to zymosan

Kazuhiro Takeuchi · Yu Umeki · Noriko Matsumoto · Kei Yamamoto · Mina Yoshida · Kazuo Suzuki · Yasuaki Aratani

Received: 17 May 2011 / Revised: 4 November 2011 / Accepted: 7 November 2011

Abstract
Objective and design This study examines the role of myeloperoxidase (MPO), a major constituent of neutrophils that generates hypochlorous acid, in neutrophil recruitment into the zymosan-exposed lung of mice.
Methods Mice were inoculated intranasally with zymosan. The accumulation of neutrophils and other inflammatory cells within the lung was analyzed by flow cytometry. Macrophage inflammatory protein 2 (MIP-2) expression in the lung was quantified, and the contribution of this chemokine to neutrophil accumulation was examined by intranasal administration of MIP-2 antibody. The cellular sources of MIP-2 were identified, and the production of this chemokine from macrophages and neutrophils was quantified in vitro.
Results Zymosan exposure led to greater neutrophil infiltration into the lungs of $MPO^{-/-}$ mice relative to wild-type mice. This was associated with higher MIP-2 levels in the mutant mice. Neutralization of MIP-2 in vivo significantly reduced neutrophil infiltration. Neutrophils from $MPO^{-/-}$ mice produced more MIP-2, and the production was reduced when MPO was added exogenously.
Conclusions MPO deficiency results in severe lung inflammation in mice exposed to zymosan. Relatively high MIP-2 levels likely contribute to the strong inflammatory response in these animals.

Keywords Inflammation · Myeloperoxidase · Neutrophil · Zymosan

Responsible Editor: Michael Parnham.

K. Takeuchi · Y. Umeki · N. Matsumoto · K. Yamamoto · M. Yoshida · Y. Aratani (✉)
Graduate School of Nanobioscience, Yokohama City University, Seto 22-2, Kanazawa, Yokohama 236-0027, Japan
e-mail: yaratani@yokohama-cu.ac.jp

K. Suzuki
Inflammation Program, Department of Immunology, Chiba University Graduate School of Medicine, Inohana 1-8-1, Chuo, Chiba 260-8670, Japan

Introduction

Neutrophil accumulation is a critical event in the pathogenesis of lung inflammation. The generation of hypochlorous acid (HOCl) by myeloperoxidase (MPO) in neutrophils is crucial to the host–defense response. We previously reported that this enzyme is essential for killing invading microorganisms in mice and that intranasal infection by *Candida albicans* and *Cryptococcus neoformans* results in a more severe pneumonia in MPO-deficient ($MPO^{-/-}$) mice than in wild-type controls [1–5].

Impaired reactive oxygen species (ROS) production by neutrophils has previously been shown to cause an abnormal inflammatory response. Mice deficient in phagocyte NADPH-oxidase, which lack the production of superoxide (O_2^-) by phagocytes, exhibit increased peritoneal leukocytosis in response to thioglycollate [6, 7]. Intratracheal administration of inactivated *Aspergillus* hyphae produced a chronic bronchopneumonia with a distinctive neutrophil infiltrate in mutant mice but not in wild-type mice [8]. The mutant mice also exhibited granulomatous synovitis and increased connective tissue destruction in an experimental arthritis model [9]. These studies suggest that an impairment in O_2^- production results in neutrophil dysfunction and causes an abnormal inflammatory response. We previously reported that neutrophils accumulate at ultraviolet

Published online: 25 November 2011

B (UVB)-exposed sites more rapidly in $MPO^{-/-}$ mice than in wild-type controls, which suggests that neutrophil-derived HOCl is a factor that can modulate neutrophil infiltration to inflammatory sites [10].

Zymosan, a β-glucan-rich cell wall preparation from *Saccharomyces cerevisiae*, has been widely used as a model of fungus-mediated inflammation, initiating phagocytosis and the production of inflammatory cytokines and chemokines [11, 12]. Intratracheal administration of zymosan has been shown to induce pulmonary inflammation in animal models [13]. It stimulates the oxidative burst in macrophages and neutrophils following internalization [14].

In the present study, we found that $MPO^{-/-}$ mice exhibit more severe pulmonary inflammation than wild-type mice when challenged with an intranasal administration of zymosan. In addition to measuring the kinetics of neutrophil accumulation, we also measured the production of macrophage inflammatory protein (MIP-2) in the lung, and we correlated the degree of neutrophil accumulation with the production of this mediator. Our results demonstrate that MPO regulates the production of MIP-2, which may modulate neutrophil accumulation during lung inflammation.

Materials and methods

Animals

Experiments on 8–12-week-old C57BL/6 mice were performed in accordance with the guidelines of Yokohama City University, Japan. C57BL/6 mice were purchased from Japan SLC (Hamamatsu, Japan). $MPO^{-/-}$ mice were generated as previously described [1]. All animals were housed under specific-pathogen-free conditions.

Induction of lung inflammation by zymosan administration

Mice were anesthetized with 2,2,2-tribromoethanol (Sigma-Aldrich). Wild-type and $MPO^{-/-}$ mice were intranasally challenged with 340 μg of zymosan (Invitrogen) in a volume of 30 μl of phosphate-buffered saline (PBS). As controls, mice were injected intranasally with 30 μl of PBS alone.

Lung histology

Mice were killed 6 days after zymosan administration, and the lungs were removed and fixed in 10% buffered formalin. For light microscopy, tissues were fixed overnight, dehydrated in graded ethanol solutions, embedded in paraffin, sectioned at 2 μm, and stained with hematoxylin/eosin (H&E) using standard protocols. Five well-separated cross-sections were analyzed by light microscopy.

Bronchoalveolar lavage (BAL) fluid preparation and immunocytochemistry

Lungs were lavaged in situ with 30 ml of PBS containing 1 mM EDTA. The BAL fluid suspensions were pooled and kept on ice until centrifugation at 1,200 rpm for 5 min at 4°C, and the resulting cell pellets were re-suspended in PBS. Total cell counts were determined using a hemocytometer. Cells were preincubated with FcR blocking antibody (anti-CD16/CD32, clone 2.4G2) to reduce non-specific binding. FITC-conjugated anti-GR1 (Ly-6G) was used to characterize pulmonary neutrophils. FITC-conjugated anti-CD11c (HL3) and PE-conjugated anti-I-A^b (AF6-120.1) antibodies were used to identify mouse macrophage and dendritic cell (DC) populations. Macrophages were defined as CD11c-positive and MHC class II-negative cells. DCs are defined as cells positively stained for both CD11c and MHC class II. The following antibodies were used to label mouse T-cell subpopulations: FITC-conjugated anti-CD4 (GK1.5), PE-conjugated anti-CD8 (H35-17.2), and FITC-conjugated anti-CD3 (17A2) monoclonal antibodies. FITC-conjugated anti-B220 (RA3-6B2) was used to characterize B-lymphocytes. All antibodies were obtained from BD Pharmingen. The cells were incubated with monoclonal antibodies for 15 min at 4°C, then analyzed on a JSAN cell sorter (Bay Bioscience, Kobe, Japan).

Measurement of MIP-2 levels

At various time points following the zymosan challenge, lungs were harvested and homogenized in PBS in the presence of protease inhibitors (Complete Protease Inhibitor Cocktail Tablets; Sigma-Aldrich). The homogenates were centrifuged at 19,000*g* for 10 min to remove cell debris. The supernatants were frozen at −80°C until assayed. MIP-2 quantification was performed using a murine MIP-2 ELISA kit (R&D Systems) according to the manufacturer's instructions. Results were expressed as mean ± SD. The detection limit of the assay was 1.5 pg/ml, as determined by the manufacturer.

Effect of anti-MIP-2 antibody on neutrophil migration induced by zymosan

Half an hour before the zymosan challenge, mice were injected intranasally with a control immunoglobulin G (IgG) (5 μg/lung, R&D Systems) or a monoclonal IgG against MIP-2 (10 μg/lung, R&D Systems). Neutrophil migration into the alveoli was measured 1 and 4 days after zymosan administration.

Intracellular cytokine staining

Standard intracellular cytokine staining was performed as follows: cells were first extracellularly labeled with FITC-conjugated anti-Gr-1, then fixed and permeabilized with BD Cytofix/Cytoperm solution (BD Pharmingen). The cells were subsequently incubated with anti-MIP-2 (R&D Systems) followed by incubation with PE-conjugated anti-rat IgG (R&D Systems). Samples were analyzed on a JSAN cell sorter.

In-vitro stimulation of macrophages and neutrophils with zymosan

Approximately 10 ml of BAL fluid was harvested per mouse, resulting in the isolation of 2.5–5 $\times$ 10^5 macrophages per animal. The alveolar cells were washed with RPMI 1640 medium (Nissui Pharmaceutical, Tokyo, Japan), followed by cell counting and differential cell analysis. More than 90% of the cells present in BAL fluid were macrophages in both wild-type and $MPO^{-/-}$ mice. Macrophages were cultured at a concentration of 1 $\times$ 10^5 cells/ml in RPMI 1640 medium supplemented with 10% fetal bovine serum (FBS) for 6 h in a 96-well culture plate (Nalge Nunc International), in the presence or absence of 200 μg of zymosan.

Bone marrow from donor mice was harvested from femora. Neutrophils were purified using a 3-layer Percoll gradient (72, 62, and 52%, Sigma-Aldrich), and washed twice with PBS. Approximately 85% of the isolated cells were morphologically identified as neutrophils by Diff-Quick (Sysmex) in both wild-type and $MPO^{-/-}$ mice. The isolated neutrophils were then cultured at a concentration of 3 $\times$ 10^5 cells per ml in RPMI 1640 medium supplemented with 10% FBS for 6 h in a 96-well culture plate in the presence or absence of 200 μg of zymosan. In some experiments, purified human MPO (0.1 unit, Sigma-Aldrich) was simultaneously added to the cells. The dose of MPO chosen was based on our previous study [15] showing that the MPO activity of mouse neutrophils was 0.41 U/2 $\times$ 10^6 cells. MIP-2 quantification was measured with ELISA kits as described above.

Determination of mitochondrial transmembrane potential ($\Delta\Psi$)

Neutrophils were incubated for 15 min at 37°C with Mito-Tracker Red CMXRos (200 nmol/L, Lonza), and the fluorescence was analyzed in a JSAN cell sorter.

Statistical analysis

Data are presented as mean ± SD. Statistical comparison between two groups was performed with a two-tailed Student's unpaired *t* test. One-way ANOVA and post-hoc Bonferroni test was performed for multiple comparisons. $P < 0.05$ was considered statistically significant.

Results

Development of lung inflammation after intranasal zymosan administration

To observe whether zymosan had any effect on lung pathology, we examined H&E-stained lung sections from wild-type and $MPO^{-/-}$ mice. Lungs from untreated mice showed negligible or minimal signs of inflammation in both wild-type (Fig. 1a, panel a) and $MPO^{-/-}$ mice (panel c). The lungs of wild-type mice at 6 days after zymosan administration showed only localized areas of inflammation (panel b). In contrast, there was prominent airway accumulation of inflammatory cells, which frequently became confluent, in the $MPO^{-/-}$ mice (panel d and e).

There were obvious differences in the total number of BAL fluid cells between wild-type and $MPO^{-/-}$ mice following zymosan exposure (Fig. 1b). In wild-type mice, the number of total cells increased, peaking 3 days after treatment and decreasing thereafter. In comparison, a much greater cellular influx was observed at days 1 through 6 in $MPO^{-/-}$ mice, and an approximately fourfold greater number of cells had accumulated by day 6. Treatment of both wild-type and $MPO^{-/-}$ mice with the PBS control had no effect on cell number (data not shown).

The various cell types present in BAL fluid were measured at 6 days post-zymosan injection (Table 1). The number of alveolar macrophages ($CD11c^+$/I-A^{b-}) did not change significantly. Although zymosan treatment resulted in a slight increase in the number of infiltrating $CD4^+$ and $CD8^+$ T cells, B cells ($B220^+$), and DCs ($CD11c^+$/I-A^{b+}), there was no significant difference in the number of those cells between wild-type and $MPO^{-/-}$ mice. Neutrophils were identified by the expression of a granulocyte marker, Gr-1. Among the Gr-1^+ cells, Gr-1^{high+} cells mostly showed morphology with polymorphous or ring-shaped nuclei (see Fig. 4b), indicating that these cells were neutrophils. The Gr-1^{high+} neutrophils were the most predominant cell type in both wild-type and $MPO^{-/-}$ alveoli, which indicates that intranasal administration of zymosan causes neutrophil-mediated lung inflammation, and that the lack of MPO enhances neutrophil accumulation.

MIP-2 is involved in zymosan-induced neutrophil migration

To gain insight into the molecular mechanisms of zymosan-induced lung inflammation, protein levels of MIP-2 in

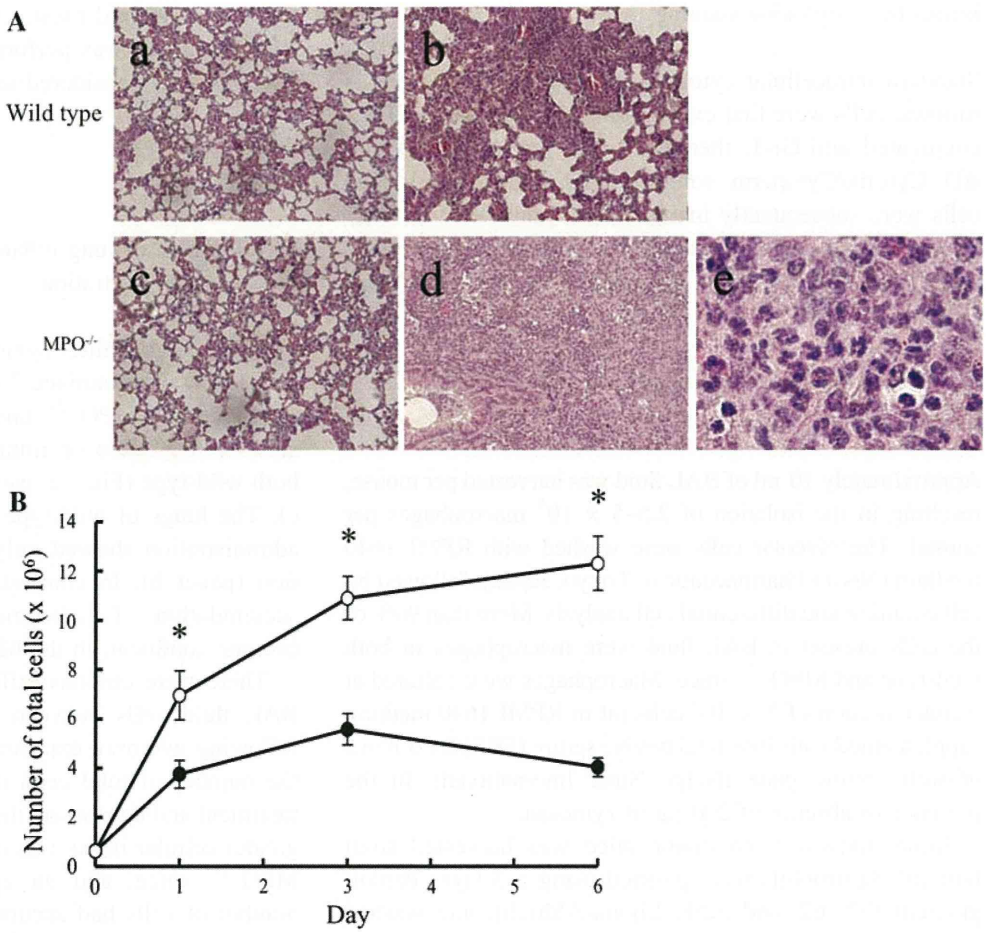

Fig. 1 **a** Lung pathology observed in mice 6 days after intranasal administration of zymosan. Lung tissues were obtained from wild-type (**a**, **b**) and $MPO^{-/-}$ (**c**–**e**) mice exposed to 340 μg zymosan for 6 days (**b**, **d**; ×10). Lung sections not exposed to zymosan (**a**, **c**; ×10) were also stained with H&E as a control. Higher magnification (×100) of the same section as *panel* **d** is shown in *panel* **e**. **b** Number of BAL fluid cells recovered from the lung after intranasal inoculation with zymosan. Wild-type (*black circles*) and $MPO^{-/-}$ mice (*white circles*) were inoculated intranasally with zymosan and analyzed on days 0, 1, 3, and 6. Five mice were used for each group. Results represent mean ± SD. *$P < 0.005$ compared to wild-type exposed mice

Table 1 Cell-surface markers expressed on the exudated cells from wild type and $MPO^{-/-}$ mice on day 6 of zymosan instillation

Antibody markers	Cells expressing cell surface marker, ($\times 10^6$)			
	Sham		Day 6	
	Wild type ($n = 5$)	$MPO^{-/-}$ ($n = 5$)	Wild type ($n = 5$)	$MPO^{-/-}$ ($n = 5$)
$Gr\text{-}1^{high+}$	ND	ND	2.63 ± 0.43 (64.7)	10.4 ± 1.2 (84.5)*
$CD11c^{+}/I\text{-}A^{b-}$	0.43 ± 0.08 (100)	0.50 ± 0.07 (100)	0.63 ± 0.13 (15.5)	0.83 ± 0.22 (6.8)
$CD11c^{+}/I\text{-}A^{b+}$	ND	ND	0.21 ± 0.11 (5.3)	0.40 ± 0.29 (3.3)
$CD4^{+}$	ND	ND	0.17 ± 0.10 (4.2)	0.20 ± 0.04 (1.6)
$CD8^{+}$	ND	ND	0.26 ± 0.09 (6.3)	0.26 ± 0.07 (2.1)
$B220^{+}$	ND	ND	0.16 ± 0.07 (4.0)	0.22 ± 0.10 (1.7)
$NK1.1^{+}$	ND	ND	ND	ND

Mice were exposed to zymosan. On day 6 post-zymosan, BAL cells recovered were incubated with antibodies described in the table, and were analyzed by flow cytometry. Data are expressed as mean ± SD. Values in parentheses indicate percentage of the number of each cell types among the total cells

ND not detected

* $p < 0.005$ compared to wild-type value

lung homogenates were determined 6 h, 1, and 6 days following injection. A strong and significant increase in the amount of MIP-2 was observed by 6 h, followed by a decrease (Fig. 2). Strikingly, MIP-2 levels were approximately threefold higher in the lungs of $MPO^{-/-}$ mice compared to those of wild-type mice, at both 6 h and 1 day after zymosan treatment.

The involvement of MIP-2 in zymosan-induced neutrophil migration into the lung was investigated using specific antibodies. $MPO^{-/-}$ mice were administered anti-

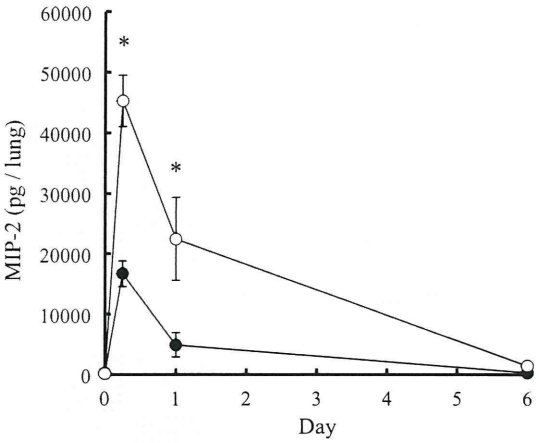

Fig. 2 Production of MIP-2 in the lungs of wild-type and $MPO^{-/-}$ mice after zymosan exposure. Lung tissues were collected and homogenized on days 0, 1, and 6 from wild-type (*black circles*) and $MPO^{-/-}$ (*white circles*) mice. MIP-2 levels were measured using specific ELISA kits. The detection limit of the assays was 1.5 pg/ml. The data are means ± SD of the results from five different mice. $*P < 0.005$ compared to wild-type mice

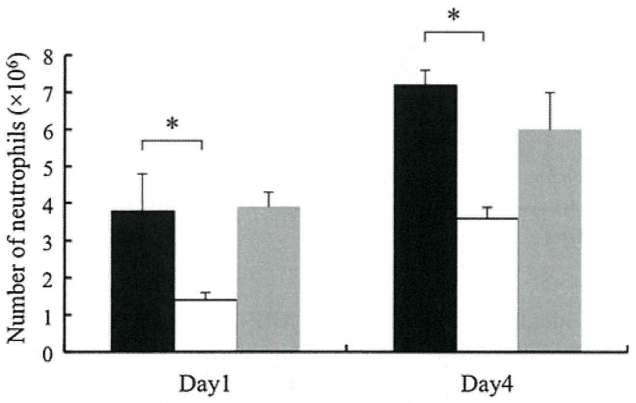

Fig. 3 Effect of anti-MIP-2 antibody on the development of lung inflammation. $MPO^{-/-}$ mice were injected intranasally with PBS (*black bars*), anti-MIP-2 antibody (*white bars*), or control rat IgG (*gray bars*) 30 min before zymosan challenge. BAL fluid cells were recovered from the mice 1 or 4 days after zymosan administration, and the number of Gr-1^{high+} neutrophils was determined using a flow cytometer. The data are means ± SD of the results from five different mice. $*P < 0.01$ compared to wild-type mice

MIP-2 antibody intranasally 30 min prior to zymosan treatment, and the number of neutrophils infiltrating into the alveoli was determined 1 and 4 days later. Treatment with the antibody resulted in a marked and significant reduction of the number of BAL fluid neutrophils harvested at 1 and 4 days (Fig. 3), strongly suggesting that MIP-2 produced by the lung contributes to neutrophil infiltration. There was no effect of control IgG as no significant change in neutrophil infiltration was observed. Taken together, these results suggest that the neutrophil-mediated inflammation observed following zymosan treatment is, at least partly, dependent on MIP-2, and that a higher production of MIP-2 in the lungs of $MPO^{-/-}$ mice contributes to the severe inflammation.

Generation of MIP-2 by macrophages and neutrophils

There is abundant evidence that lung inflammation is due to activation of lung phagocytic cells, which produce numerous chemokines [16]. To address this issue, we examined the intracellular expression of MIP-2 in Gr-1^{+} cells at the early stage of zymosan treatment. In order to characterize the Gr-1^{+} cells, the Gr-1^{high+} and Gr-1^{low+} cells were sorted from BAL fluid cells at 6 h post injection. The sorted cells were observed under a microscope. As shown in Fig. 4b, the sorted Gr-1^{low+} cells showed a mononuclear morphology, which were probably macrophages. In striking contrast, Gr-1^{high+} cells mostly showed morphology with polymorphous or ring-shaped nuclei, indicating that these cells were neutrophils. As shown in Fig. 4a, alveolar macrophages of both wild-type and $MPO^{-/-}$ mice began to express MIP-2 as early as 3 h after zymosan treatment, and continued to express it until 6 h, but then declined to undetectable levels at 72 h. The MIP-2-expressing neutrophil proportion appeared as early as 3 h and strongly at 6 h, and then decreased by 72 h. These results indicate that both alveolar macrophages and infiltrating neutrophils, at least partly, contribute to the early-phase production of MIP-2 in zymosan-challenged lungs.

We determined the generation of MIP-2 in vitro in isolated macrophages and neutrophils. Analysis of supernatants of the cultured macrophages demonstrated that the production of MIP-2 was significantly increased by zymosan treatment (Fig. 5a), indicating that the alveolar macrophages are a source of MIP-2 in lungs exposed to zymosan. Strikingly, stimulation of $MPO^{-/-}$ neutrophils with zymosan in vitro for 6 h led to a threefold greater production of MIP-2 compared to wild-type neutrophils (Fig. 5b). After culture with zymosan, >85% of the cells maintained high levels of $\Delta\Psi$ in both wild-type and $MPO^{-/-}$ neutrophils, as indicated by the strong mitochondrial staining with CMXRos dye (Fig. 5c). These results strongly suggest that stimulation of mouse neutrophils with zymosan for 6 h scarcely affects the viability irrespective of genotype for MPO.

To confirm the involvement of MPO in MIP-2 production from neutrophils, we examined the effect of exogenously added MPO enzyme on MIP-2 production. As shown in Fig. 6, addition of human MPO to MPO-deficient mutant neutrophils treated with zymosan could significantly decrease the production of MIP-2, strongly suggesting that MPO inhibits the production of MIP-2 from the zymosan-activated neutrophils.

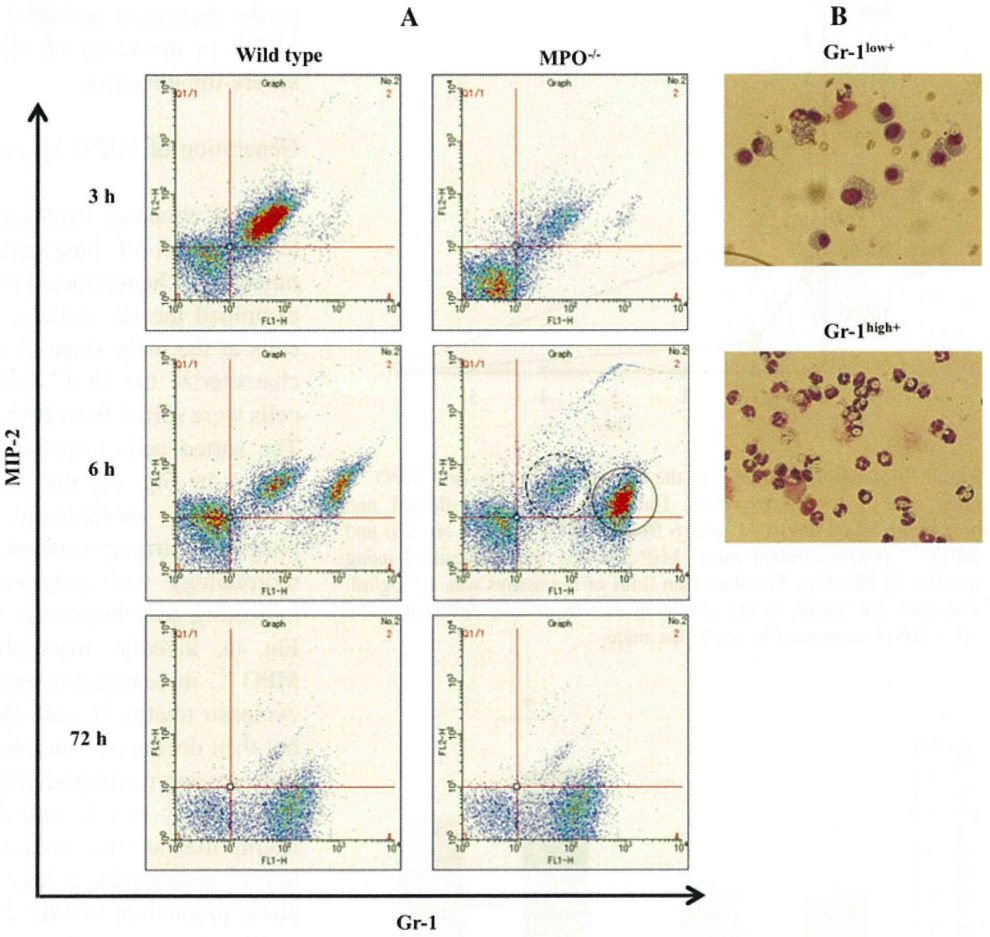

Fig. 4 Cellular sources of MIP-2 production in the lungs of zymosan-exposed mice. Mice were injected intranasally with zymosan. At the indicated time points, lung leukocytes were recovered and stained with PE-anti-MIP-2 and FITC-Gr-1 antibodies (**a**). The stained cells were analyzed by means of flow cytometry for the expression of MIP-2. A representative result of three independent experiments is shown. **b** Gr-1^{low+} cells (*dashed circle* shown in *panel* **a**) and Gr-1^{high+} cells (*solid circle* shown in *panel* **a**) sorted from the BAL fluid cells of $MPO^{-/-}$ mice at 6 h were analyzed for their morphology

Discussion

This paper describes the involvement of MPO in the zymosan-induced recruitment of neutrophils. Our data demonstrate that the lack of MPO results in severe inflammation accompanied by neutrophil infiltration. This inflammatory response in $MPO^{-/-}$ mice lung was associated with an increase in MIP-2 levels. These results suggest that MPO deficiency exaggerates zymosan-induced lung inflammation by inducing the production of MIP-2.

To understand the mechanism by which neutrophils deficient in MPO accumulate largely at zymosan-exposed sites, we first determined the concentration of MIP-2 produced in the lung. We found that MIP-2 levels in $MPO^{-/-}$ mice were significantly higher than in wild-type mice (Fig. 2), and that neutralization of this chemokine by an anti-MIP-2 antibody led to reduced lung inflammation (Fig. 3). This strongly suggests that the greater amount of MIP-2 produced in the mutant mice is involved in the higher amount of neutrophil infiltration in lung exposed to zymosan.

Several cell types, including macrophages [17], epithelial cells [18], mast cells [19], and neutrophils [20–22] have been identified as sources of MIP-2. Our results clearly indicate that both alveolar macrophages and infiltrating neutrophils are sources of MIP-2 in both wild-type and $MPO^{-/-}$ mice at an early stage (up to 6 h) following zymosan treatment (Fig. 4). Interestingly, neither macrophages nor neutrophils produced this chemokine at 72 h. These results correlate well with the observation that MIP-2 levels rapidly decreased after 6 h (Fig. 2). It is thought that the phagocytosis of zymosan results in cellular activation. Indeed, we observed that both macrophages and neutrophils, recovered from BAL fluid at 6 h, had phagocytosed zymosan (data not shown). Furthermore, none of those cells recovered at 72 h contained zymosan, perhaps due to a lack of zymosan in the lung.

Intriguingly, we found that $MPO^{-/-}$ neutrophils produced larger amounts of MIP-2 than did the neutrophils from wild-type animals, in vitro, in response to zymosan (Fig. 5b), and that addition of purified MPO enzyme reduced the production of this chemokine (Fig. 6). These data indicate that MPO deficiency up-regulates the production of MIP-2 from neutrophils. Since an early initial secretion of MIP-2 can promote the recruitment of additional neutrophils, the greater production of this chemokine